Origins of strandline duricrusts around the Makgadikgadi Pans (Botswana Kalahari) as deduced from their chemical and isotope composition

S. Ringrose [a,*], C. Harris [b], P. Huntsman-Mapila [a], B.W. Vink [c], S. Diskins [a,c], C. Vanderpost [a], W. Matheson [d]

[a] Harry Oppenheimer Okavango Research Centre, University of Botswana, Private Bag 285, Maun, Botswana
[b] Department of Geological Sciences, University of Cape Town, Rondebosch 7701, South Africa
[c] Department of Geology, University of Botswana, Private Bag 0022, Gaborone, Botswana
[d] Sunart (Pty) Ltd, Maun, Botswana

ABSTRACT

Trace elements together with some O and C isotope analysis were undertaken on duricrust strand line deposits in the palaeo-Makgadikgadi sub-basin (PMSB) to provide insight into palaeo–climatic conditions through the interpretation of calcrete, silcrete–calcrete intergrade and silcrete deposits. Trace element content and relative abundance suggest that the duricrust origins are associated with the long-term weathering of the Karoo Large Igneous Province which underlies the PMSB. This work shows that duricrust origins are related to Ca^{2+} and Si (and associated trace elements) being transported mainly through the groundwater and then subsequently precipitated at different strandline elevations over time. Local groundwater feeding in towards the pan margin and accumulating in near-neutral pan-marginal pools, appears to facilitate Si concentration and permeation of pre–existing calcretes. The silica precipitates as the pH drops when renewed freshwater enters the pools. Hence the inferred palaeo-climatic regime for silcretisation may be similar to that occurring in Botswana at present being dry semi-arid with low seasonal rainfall. In contrast the extensive calcrete precipitation in the strandlines results from abundant Ca^{2+} in adjacent waters which appear to be derived from both local and regional sources. The arrival of Ca^{2+} from regional sources (shown by trace element evidence) infers heavy rainfall in the upper catchment suggesting a major humid event followed by regional drying. Palaeo-climatic inferences suggest the juxtaposition of major humid events interspersed with more normal semi-arid palaeo-climates with an exception obtained from isotope data, of drier and cooler conditions than usual for the region around 80–90000 years ago. Whereas trace element data can greatly assist in the interpretation of complex deposits such as duricrusts, care should be taken over the use of particular ratios (such as Yb/Gd ratio) which may produce spurious results.

Keywords:
Kalahari duricrusts
Calcretisation
Silcretisation
Silcrete–calcrete intergrade deposits
Palaeo-climatic change

1. Introduction

Element compositions of calcareous sedimentary rocks can greatly aid the interpretation of their origins (Wolf et al., 1967). Carbonate rocks in general have attracted considerable attention in this regard with a number of researchers developing indicators for palaeo-temperature, salinity and weathering (e.g. Chilingar, 1963; Fairbridge, 1964; Huntsman-Mapila et al., 2006). A number of analyses are now available as a result of the increasing use of calcrete in geochemical prospecting (e.g. Davies and Jenkins, 2003). Calcretes are often permeated by silica to form silcrete–calcrete intergrade deposits which have been reported (as such) in southern Africa, although they likely occur extensively in semi-arid areas worldwide (Nash and Shaw, 1998; Ringrose et al., 2002, 2005; Nash et al., 2004; Kampunzu et al., 2007). Calcareous duricrusts are potentially good palaeo-climatic indicators and their $\delta^{13}C$ and $\delta^{18}O$ values coupled with dating techniques can be used to document climatic variations during the Quaternary (Amundson et al., 1994; Wang et al., 1994; Nash et al., 1994; Monger et al., 1998; Buck and Monger, 1999; Deutz et al., 2001). Ringrose et al. (2005) and Kampunzu et al. (2007) used geochemical data from both calcretes and silcrete–calcrete intergrade deposits to infer palaeo-climates in the PMSB (palaeo-Makgadikgadi sub-basin) and the Moshaweng valley. Whereas a genetic link between calcretes and silcretes may be inferred by their field relationships (Thomas and Shaw, 1991; Summerfield, 1983a,b; Ringrose et al., 1999, 2002; Nash et al., 2004) the processes involved in the deposition of silcrete–calcrete intergrade deposits and associated calcretes and silcretes are not fully understood. Further work is therefore required to clarify their origins in terms of the porewater conditions under which precipitation occurs and to therefore infer a broader palaeo-climatic sequence for the PMSB.

This work considers duricrust deposition in the peripheral sands of the palaeo-Makgadikgadi Pans which represent a zone of convergence of surface and groundwater likely derived from an extensive sub-tropical catchment (cf. Moore and Larkin, 2001). Rain and surface inflow water have evaporated over time to form the highly (chloride dominant) saline sub-pan groundwater (Gould, 1986) but the surface water of the pans varies between fresh (following rains) and highly

* Corresponding author. Tel.: +267 6817222; fax: +267 6861835.
E-mail address: sringrose@orc.ub.bw (S. Ringrose).

alkaline–saline water (during the subsequent dry season). Duricrusted strandlines occur intermittently above the pan surface which occurs around 890 m. The strandlines have been surveyed to elevations between 904 m and 945 m (Cooke and Verstappen, 1984) and on the basis of stone tools, may date back to over 200 000 years (McFarlane and Segadika, 2001). The duricrusts result from multiple phases of calcretisation and subsequent silcretisation as precursor calcretes show evidence of overprinting (Ringrose et al., 2005). Beds of pure silcrete although also considered in this work, are relatively rare in the strandlines. The present work aims to: 1) determine how trace elements in PMSB duricrusts can help to explain the nature of calcretisation and silcretisation events; 2) indicate how isotope analysis can extend the results obtained and help explain exceptional events, and 3) by extending porewater conditions to the larger environment, consider how the results may enhance the interpretation of palaeo-climates during the Late Quaternary in the region.

2. Geological and hydrogeological setting

The study area forms part of a down-faulted graben in north-eastern Botswana (Tiercelin and Lezzar, 2002). The entire palaeo-flooded area is referred to as palaeo–Makgadikgadi sub-basin (PMSB) which lies between 19.80S–21.60S and 25.75E–26.40E covering approximately 27 600 km^2 (Fig. 1). The PMSB is sparsely vegetated with exposed salt encrusted surfaces surrounded by grassland. The area has an anomalously low rainfall at ~400 mm/year (Ringrose and Matheson, 2003) with high seasonal and diurnal temperature ranges (48 °C summer daytime to 3 °C winter night time). At present precipitation is exceeded by evapo-transpiration by a factor of three (Bhalotra, 1987). The PMSB circumscribes Sua Pan in the east and Ntwetwe Pan in the west. Bedrock geology comprises mainly Karoo Formations (Lebung and Ecca sandstones and Thlabala shales) with younger Karoo volcanics to the north (Geological Survey of Botswana, 2000) (Fig. 2). These units are crossed by the giant ESE–WNW trending doleritic dyke swarm (Jourdan et al., 2004), which is part of the Karoo Large Igneous Province. Many dykes are exposed along the pan margins and have been dated at ~187 Ma (Elburg and Goldberg, 2000).

The present work concentrates on duricrusts occurring towards the northern end of Sua Pan (Fig. 3). The pan is infilled with fine-medium sand (the brine aquifer) overlain by interbedded sand and clay to a depth of ~80 m (Gould, 1986). A sub-pan caustic (alkaline) brine of the Na (K)–Cl–CO_3–HCO_3–(SO_4) type is being pumped for NaCl and soda ash production (Molwalefhe, 2003) in the vicinity of Sua spit (Fig. 3). The PMSB receives drainage from three major catchments which drain mainly through regolith comprising the Kalahari Group sequence (Fig. 4). The local Kalahari Group sediments are documented in Thomas and Shaw (1991) and more specifically in Du Plessis (1993). Most inflowing rivers are assumed to have been considerably more active during past humid intervals (Shaw and Thomas 1992; Thomas and Shaw, 2002) but their waters have mostly evaporated leaving the brine concentrate. Sua Pan is the lowest member of the sequence with a sump level of 890 m a.s.l. The pans are surrounded by discontinuous strandlines ranging in elevation from 904 m to 945 m a.s.l. (Thomas and Shaw, 1991, and references therein) who along with Ringrose et al. (2005) interpreted the strandlines as shorelines peripheral to palaeo-lake Makgadikgadi.

3. Sampling, petrography and analytical methods

The duricrust strandlines were examined at eleven locations which vary in elevation from 945 m (≈50 m above the present pan floor) to 904 m close to the present pan margin. The strandlines were examined in detail in road-cuts and borrow pits (Fig. 3). Details of the duricrust profiles along with approximate TL/OSL ages from Ringrose et al. (2005) are shown on Table 1. Care while sampling facilitated the differentiation between the compound duricrust types comprising for instance silcrete–calcrete intergrade lithoclasts, which were visually distinct from the surrounding calcrete. Preliminary analyses indicated that most of the profiles comprised silcrete–calcrete intergrade deposits often

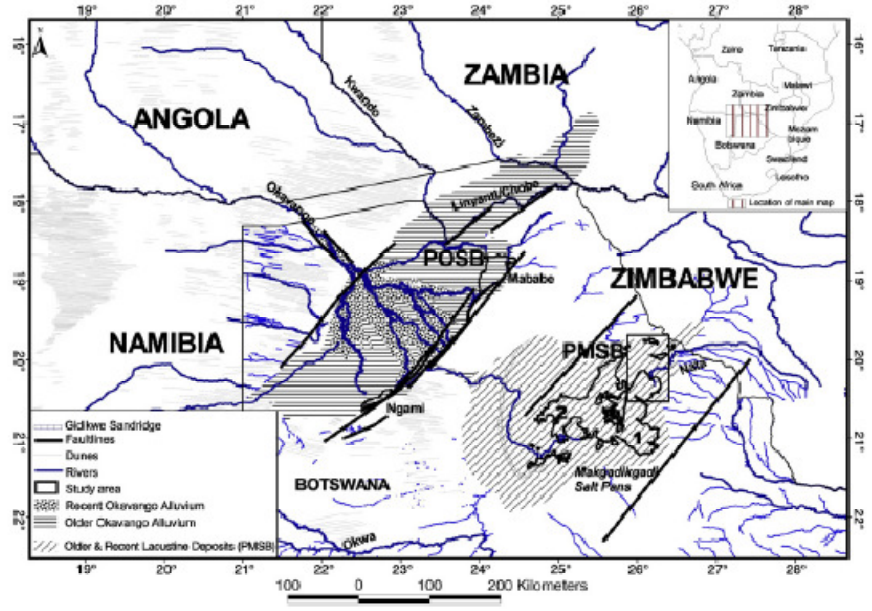

Fig. 1. Location of the MOZ (Makgadikgadi–Okawango–Zambezi rift depression (southern extension of the East African Rift) subdivided into the palaeo-Makgadikgadi sub-basin (PMSB) and palaeo-Okavango sub-basin (POSB) in northern Botswana.

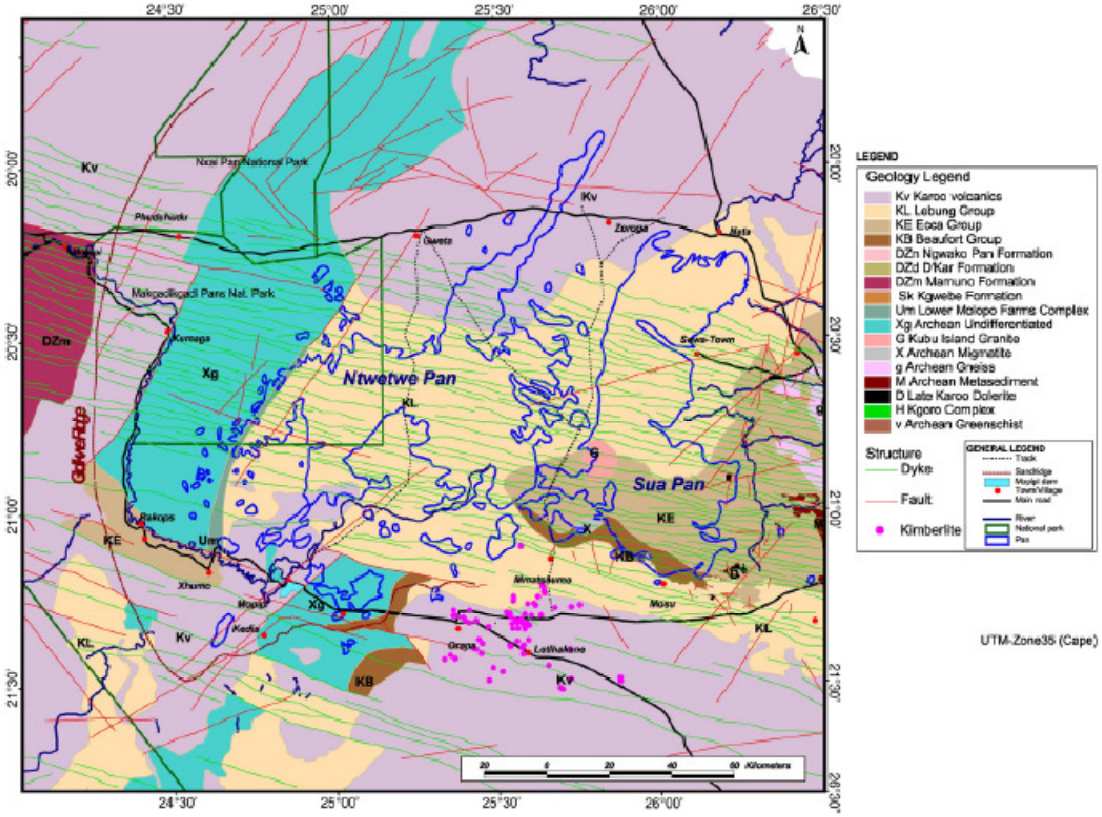

Fig. 2. Distribution of major geological formations including dyke swarms in the PMSB (after Botswana Geological Survey, 2000).

embedded in a later calcrete, with relatively un-altered calcretes occurring predominantly in the 936 m strandline. Samples from each location comprised minor silcretes and silcrete–calcrete intergrade deposits from the 943–945 m strandline, calcretes from the 936 m strandline, and mostly intergrade deposits from the lower strandlines (Table 1). These samples were examined in hand specimen and thin section prior to XRD, ESEM and major element geochemical analyses. The results (Fig. 8, Ringrose et al., 2005) revealed that the intergrades comprised precursor calcretes permeated by thin veins and coats of silica and are therefore displacive rather than replacive. Ringrose et al. (2005) also indicated that the strandline duricrusts were divisible into four main types based on $CaCO_3$ and SiO_2 content (Walker, 1960; Summerfield, 1983a,b; Nash and Shaw, 1998). Specifically, the calcretes contained between 60–80 wt.% calcite and 10–30 wt.% SiO_2 and were found throughout the SOW1 profile at 936 m and the basal units of SOW10 and SOW7A/13. Two silcrete–calcrete intergrade deposit types were identified with compositions between 35–50 wt.% calcite and 35–52 wt.% SiO_2, and between 15–30 wt.% calcite and 58–72 wt.% SiO_2. Because of their similar origins, these are combined in the present work as one major silcrete–calcrete intergrade type (Nash and Shaw, 1998 as redefined in Nash et al., 2004). The silcretes contained between <10 wt.% calcite and 78–95 wt.% SiO_2.

Whole rock chemical analysis was performed on twenty-five selected samples from each of the major units at Chemex Canada Ltd. The samples analysed comprised mostly lithoclasts considered to be representative of multiple calcretisation or calcretisation/silcretisation events (Table 1). Major element compositions, discussed in Ringrose et al. (2005) were determined using an ICP-AES with a detection limit of 0.01 wt.% with a relative precision of ±1% (Kane, 1992; Thompson, 1992). Trace elements including REEs were analysed using an ICP-MS with lower detection limits between 0.01 and 0.5 ppm depending on the element under consideration (Thompson, 1992). Similar techniques are described at length in Ødegard (1997) which includes a full description of the lower detection limits and precision values. Li, Cr, Ni and Pb were determined by flame AAS with a detection limit of 1 ppm. The precisions are ±5% for trace elements between 0.01 and 10 000 ppm. (Taylor, 1987; Ødegard, 1997). To determine the F content, a sample was fused with a 2:1 sodium carbonate and potassium nitrate mixture. The melt was leached with water and citric acid added to adjust the pH to 5.5. The fluoride activity was measured with a specific ion electrode. Chloride analysis was undertaken by KOH fusion then determined using a specific ion electrode. Loss on Ignition (LOI) analysis involved placing a 1.0 g sample in an oven at 1000 °C for 1 h. The sample was later cooled and then weighed. The percentage LOI was calculated from the difference in weight. Inorganic CO_2, and total CO_2 content were determined using a Leco-Gasometric and Leco-IR detector with detection limits of 0.2 and 0.01 respectively. The procedure required the decomposition of samples with diluted hydrochloric acid, after which the organic carbon is separated by filtration. The residue was subsequently washed with de-ionized water, dried and placed in the Leco-IR detector. Hence the organic carbon (and the generated CO_2) were quantitatively detected by infrared spectrometry and reported as percentages (e.g. Ødegard, 1997).

Carbon and oxygen isotope ratios were determined after verifying the mineralogy by X-ray diffractometry. Stable isotope measurements

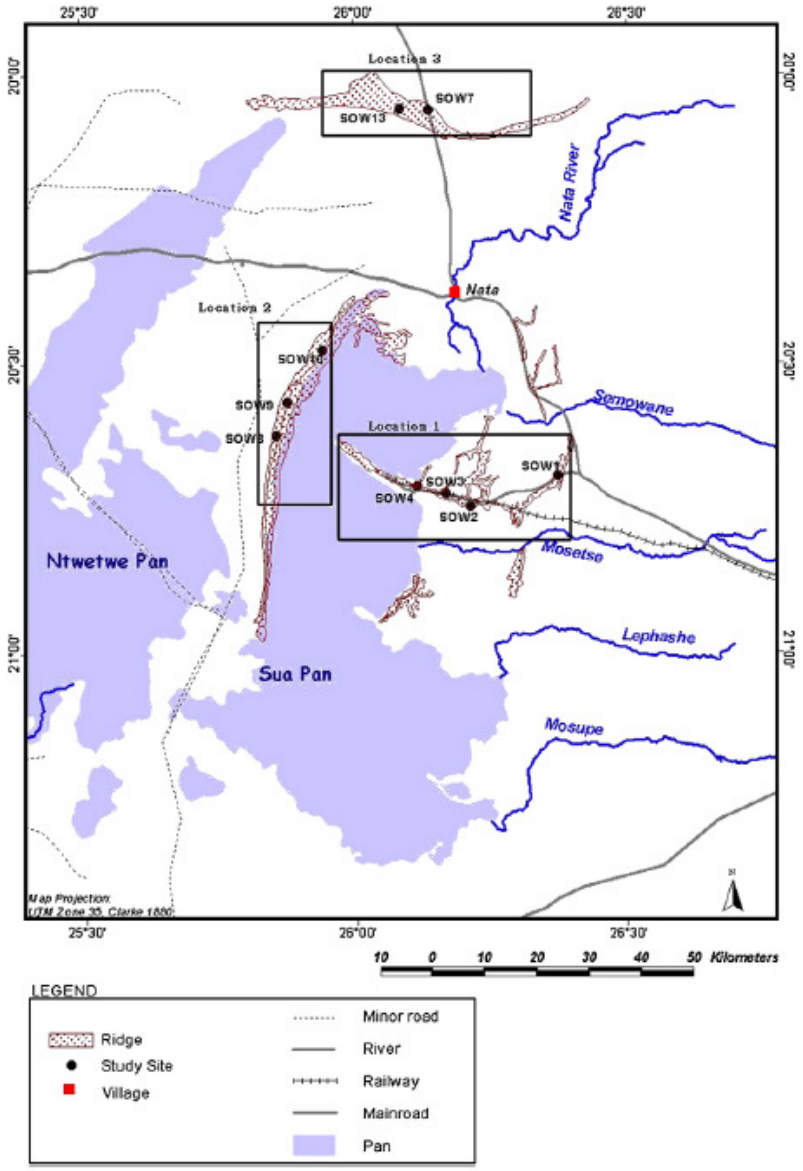

Fig. 3. Location of PMSB strandlines peripheral to northern Sua Pan and sample locations examined in the field (after Ringrose et al., 2005). Strandline elevations shown at 945 m, 936 m, 924 m, 906 m and 904 m.

were made at the University of Cape Town (UCT) on powdered calcrete samples. The calcretes contain calcite as the dominant carbonate mineral with small amounts of dolomite occurring in only one sample. The CO_2 was therefore extracted by reaction of 3–10 mg of powered sample and 5 ml of 100% H_3PO_4 at 25 °C using the classical method of McRae (1950). The CO_2 extracted from the calcite samples was analysed for both carbon and oxygen using a Finnegan MAT Delta XP mass spectrometer in dual inlet mode, and the data were corrected using the CO_2–calcite fractionation factor of 1.01025. Data are reported in the familiar δ notation where $\delta = (R\text{sample}/R\text{standard} - 1) * 1000$ and $R = {}^{18}O/{}^{16}O$ or ${}^{13}C/{}^{12}C$. An in-house carbonate standard, Namaqualand marble (NM), was run in duplicate with each batch of samples. The data obtained on the NM standard were used to convert the raw data to the PDB and SMOW scales. The long-term duplication of NM suggests that the precision for both $\delta^{18}O$ and $\delta^{13}C$ is better than 0.1.

4. Trace element composition

4.1. Alkali and alkali earths

Duricrust data for the alkali earths results in the Ba values for calcretes ranging between 182 and 2930 ppm, while concentrations

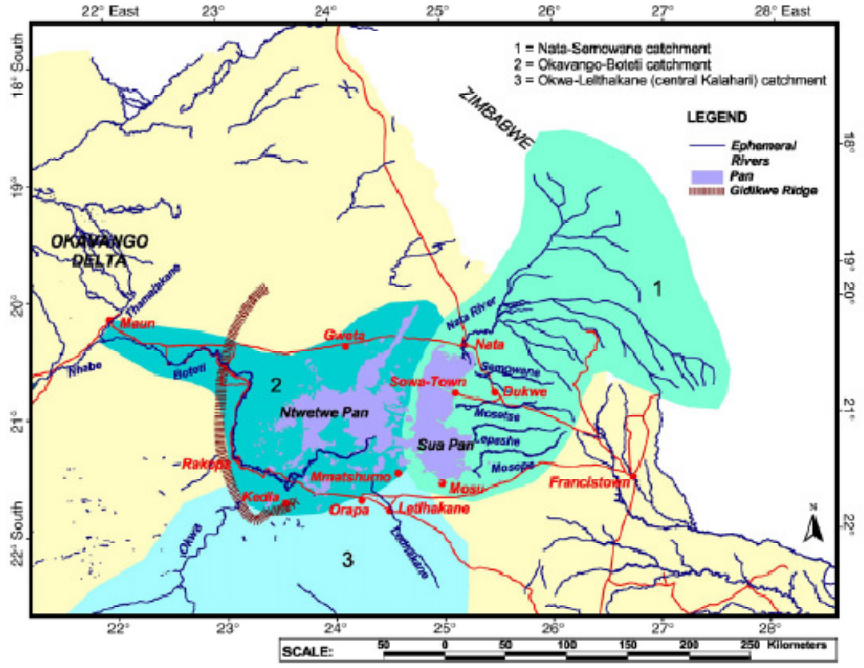

Fig. 4. Distribution of major ephemeral catchments feeding in to the PMSB (1 = Nata–Semowane catchment, 2 = Okavango–Boteti catchment, 3 = Okwa–Lethlakane, central Kalahari catchment).

for the silcrete–calcrete intergrade deposits range between 412 and 4820 ppm with a reduction for silcretes of between 191.5 and 525 ppm (Table 2). The overall Ba compositional range is from 3.5 times lower to 7.6 times higher than the Ba NASC (North American Shale Composition) value (Taylor and McClennan, 1985). Ba concentrations are also generally higher than those reported for Karoo dolerites (168–467 ppm, Elburg and Goldberg, 2000). The highest abundances are found in intergrade samples from SOW3 (924 m) where the Ba increases markedly with depth from 702 ppm to 4820 ppm. Sr concentrations range between 262 and 1080 ppm in calcretes, 442 and 5610 ppm in the intergrade deposits and between 24 and 1130 ppm in silcretes, hence Sr is particularly abundant in the intergrade duricrusts (Table 2). The overall Sr compositional range is from 0.2 times lower to 39 times higher than the Sr NASC value (Taylor and McClennan, 1985) but is comparable to, or higher than that found in the Karoo dolerites of Botswana (204–597 ppm, Elburg and Goldberg, 2000) for all duricrust types. Compared to Ba variability, a less marked increase is noted with depth in the SOW3 silcrete–calcrete intergrade deposit as the Sr content changes from 1110 ppm to 3120 ppm. Interestingly Sr and Ba abundances vary markedly throughout the strandlines such that Sr is dominant in the upper (945 m) strandlines while Ba dominates at 906 m and 924 m, while Sr is again concentrated towards the present Pan margin at 904 m (Fig. 5a). According to Wolfe et al. (1967) the relative composition of Sr or Ba is dependent on conditions in the water medium prior to precipitation suggesting that the geochemical composition of introduced porewaters peripheral to the pans also changed over time. High Ba and Sr abundances along with other elements, are depicted on Upper Continental Crust (UCC) normalized multi-element spider plots relative to the NASC reference (Figs. 5b, 6a and b) where the order of elements is according to Hoffmann (1988). The normalizing values used are from Taylor and McClennan (1985), except for Cs and Ta where average concentrations of Plank and Langmuir (1998) are preferred (cf. Kampunzu et al., 2007). Samples from different strandlines are coded by site and with S1 representing samples taken from the top of the profile to S..n towards the base. The calcretes are marked by strong positive anomalies comprising CaO, (most samples) Sr, (SOW10 S3) Ba (SOW1 S2) and U (SOW1 S6) (Fig. 5b). Silcrete–calcrete intergrade duricrust samples are also marked by similar positive anomalies for CaO, (most samples) for Sr (SOW3 S1) and Ba (SOW3 S2) (Fig. 6a). U is particularly evident at SOW13 S1A and SOW8B while Th anomalies occur at SOW13 S1 and SOW10 S2. Silcrete samples are marked by lower positive anomalies for CaO (SOW13 S3) and comprise higher (>10) Sr positive anomalies (e.g. SOW13 S2) (Fig. 6b). Rb and Li abundances are much lower than Sr and Ba, with Rb dropping to between 6.6 and 37.4 ppm for calcretes, 28.8 and 41.0 ppm for intergrade deposits and 18.8 and 73.4 ppm for silcretes. These values are 2–20 times lower than NASC concentrations for Rb (Gromet et al., 1984) (Table 2) but are comparable to published Rb values (10.7–43.4 ppm) for Karoo dolerites (Elburg and Goldberg, 2000). Li values range from 1 to 12 ppm for calcretes, 3.4 to 43 ppm for intergrades and 6 to 42 ppm for silcretes with the Li content increasing with Al_2O_3.

4.2. Transition metals and Zr

Chromium, cobalt and nickel concentrations in the duricrusts range from between 6 and 16 ppm, 3 and 11 ppm and 5 and 60 ppm respectively while other metals are low throughout (Table 2). Compared to NASC abundances, Ni concentrations are lower in the silcrete–calcrete intergrade deposits and silcretes but are generally closer to NASC abundances in calcretes from the 936 m strandlines (SOW1 S1) (Figs. 5b, 6a and b). Co abundances are between 2.3 and 8.6 times lower than those found in the NASC data set. Concentrations of V and Cu range between 10 and 95 ppm and 5 and 30 ppm respectively, with higher V concentrations in calcrete at the 936 m level (SOW1 S5–95 ppm) and higher Cu concentrations in the 924 m strandline (SOW3 S2). Background Cu, Ni and V contents tend to occur in all the other

Table 1
Profile details for duricrust from PMSB strandlines and inferred repeat periods when same strandlines incorporated more recent groundwater flow (modified after Ringrose et al., 2005, 2008).

Location and profile depth	Height above sea level (m)	Profile composition[a]	Approx. and age	Assumed origin[b]
SOW7A and 13 (m)	943–5	S1. Grey sand or laminated hardpan S2. Friable nodular silcrete–calcrete intergrade deposit with quartz pebbles S3. Friable nodular calcrete–silcrete with lithoclasts S4. Partially indurated nodular calcrete S5. Light green sand with scattered siliceous rhizoliths S6 Indurated calcrete with silcretes–calcrete intergrade lithoclasts	102.2 ka siliceous clast in hardpan 108.6 ka inner rhizolith 90.4 ka siliceous clast 83.6 and 80.7 ka nodules 41.2 ka siliceous lithoclasts	Drying interval after first humid interval >110 000 years (Lake Okavango and Zambesi flooding) Second dry interval after humid period >41–43 000 years
SOW1 (m)	2.0	936	S1. Indurated calcrete hardpan S2–3. Friable calcrete with quartz pebbles S4. Friable calcrete S5. Laminated calcrete S6. Nodular indurated calcrete	90.7 ka -lithoclast	Cold, dry interval after humid period >80–90 000 years
SOW2 3 and 4 (m)	2–3.0	912–924	S1. Indurated calcrete hardpan S2. Friable nodular silcrete–calcrete intergrade deposit with quartz pebbles S3. Moderately indurated nodular silcrete–calcrete intergrade deposit with Si-enriched lithoclasts S4. Well formed siliceous rhizoliths in green, granular calcareous matrix	43.4 ka siliceous lithoclast	Second drying interval after second humid period >41–43 000 years
SOW10 (m)	2.5	906	S1. Indurated calcareous duricrust with surface weathering S2. Brecciated silcrete–calcrete intergrade deposit with terrazzo silcrete inclusions S3. Recrystallised green calcrete with silcrete–calcrete intergrade lithoclasts	No date
SOW8A and 8B (m)	0.5	904	Uniform sand with disseminated silcrete–calcrete intergrade particles and siliceous rhizoliths	8.8 ka	Holocene drying event

[a] Evidence of desiccation cracking occurs intermittently throughout all profiles.
[b] Calcretes precipitate during dry interval following a humid period.

duricrusts (Fig. 7a). In contrast Zr values are consistently high ranging between 21.5 and 63.5 ppm for calcretes, 43.5 and 198.5 ppm for intergrade deposits and 100.5 and 220 ppm for silcretes (Table 2 and Fig. 7b). This is higher than the 10–160 ppm range found in the Olduvai calcretes (Hay and Reeder, 1978) but comparable to the Karoo dolerite range (92.3–302.2 ppm, Elburg and Goldberg, 2000), thereby adding to the plausibility of a weathering product origin for these deposits.

4.3. U, Th, W, Y and halogens

Uranium concentrations are variable ranging from 1 to 5.5 ppm in the calcretes of SOW1 and from 0.5 to 7.5 ppm in the silcrete–calcrete intergrade deposits where the highest abundance in the 904 m strandline (SOW8A) is adjacent to the present Pan shoreline (Fig. 7b). Thorium abundance is generally low in the 936 m calcretes (<1–7 ppm)

Table 2
Alkali earth and transition metal abundances in ppm from PMSB strandlines—SOW8A (904 m) to SOW7A (945 m).

Sample	Type	Ba	Sr	Rb	Li	Cs	Cr	Co	Ni	V	Cu	Pb	Tl	Zn	Sn	Zr
SOW8A	I/G	1025	2000	20.8	14.0	0.30	6.0	3.5	10.0	10.0	<5	5.0	<0.5	<5	< 1	46.5
SOW8B	I/G	1340	1445	23.2	17.0	0.40	6.0	3.0	15.0	15.0	5.0	<5	<0.5	<5	< 1	54.0
SOW10-S1	I/G	3980	1 375	22.6	10.0	0.30	10.0	4.5	15.0	15.0	5.0	5.0	0.5	5.0	< 1	198.5
SOW10-S2	I/G	3240	510	28.8	18.0	0.40	16.0	10.5	15.0	20.0	10.0	<5	1.0	5.0	< 1	115.5
SOW10-S3	C	2670	1055	15.4	10.0	0.20	8.0	3.0	10.0	15.0	15.0	10.0	0.5	<5	< 1	28.0
SOW3-S1	I/G	702	1110	28.8	13.0	0.30	10.0	4.5	15.0	10.0	10.0	<5	<0.5	5.0	< 1	43.5
SOW3-S2	I/G	1595	1630	36.2	43.0	0.40	14.0	6.5	60.0	15.0	35.0	<5	<0.5	10.0	< 1	67.0
SOW3-S3	I/G	2490	3 120	35.0	37.0	0.30	12.0	4.5	10.0	15.0	5.0	5.0	<0.5	5.0	< 1	50.0
SOW3-S4	I/G	4820	2470	32.0	31.0	0.40	12.0	5.0	10.0	20.0	<5	10.0	<0.5	5.0	< 1	61.5
SOW1-S1	C	182	262	13.6	1.0	0.30	14.0	5.0	60.0	30.0	25.0	<5	<0.5	<5	< 1	44.0
SOW1-S2	C	2930	702	7.4	1.0	0.10	10.0	10.0	30.0	45.0	30.0	5.0	<0.5	<5	< 1	30.5
SOW1-S3	C	369	874	6.6	6.0	0.10	6.0	5.0	20.0	25.0	10.0	<5	<0.5	<5	< 1	22.0
SOW1-S4	C	338	1080	10.8	6.0	0.20	6.0	5.0	15.0	40.0	10.0	5.0	<0.5	<5	< 1	57.5
SOW1-S5	C	607	847	13.0	7.0	0.20	8.0	3.5	25.0	95.0	10.0	<5	<0.5	<5	< 1	37.5
SOW1-S6	C	216	512	9.6	4.0	0.20	8.0	4.0	15.0	95.0	5.0	10.0	<0.5	<5	< 1	21.5
SOW13-S1	I/G	1455	1630	37.2	22.0	0.50	14.0	5.0	20.0	15.0	10.0	<5	0.5	5.0	< 1	131.0
SOW13-S1A	I/G	474	3050	22.2	8.0	0.30	8.0	4.0	20.0	10.0	<5	<5	0.5	<5	< 1	80.5
SOW13-S2A	I/G	412	5 610	18.8	9.0	0.30	8.0	5.5	5.0	10.0	<5	<5	2.5	<5	< 1	114.5
SOW13-S2	S	415	781	32.4	15.0	0.40	8.0	4.0	15.0	15.0	10.0	<5	<0.5	5.0	< 1	139.5
SOW13-S3	S	525	1130	37.0	18.0	0.60	10.0	5.5	10.0	15.0	<5	<5	4.0	5.0	< 1	141.5
SOW7A-S1	S	192	24	43.6	6.0	0.60	10.0	11.0	5.0	15.0	<5	5.0	<0.5	5.0	< 1	220.0
SOW7A-S3	S	415	114	73.4	42.0	1.10	18.0	11.0	15.0	25.0	<5	<5	0.5	10.0	< 1	100.5
SOW7A-S2	I/G	575	1425	41.0	19.0	0.50	10.0	6.0	10.0	15.0	5.0	5.0	<0.5	5.0	< 1	60.0
SOW7A-S2A	I/G	607	442	38.0	29.0	0.40	10.0	4.5	10.0	15.0	5.0	<5	<0.5	5.0	< 1	117.5
SOW7A-S4	C	1055	521	37.4	12.0	0.40	14.0	5.5	10.0	30.0	10.0	<5	<0.5	5.0	< 1	63.5

C = Calcrete, S = Silcrete, I/G = silcrete–calcrete intergrade deposit.

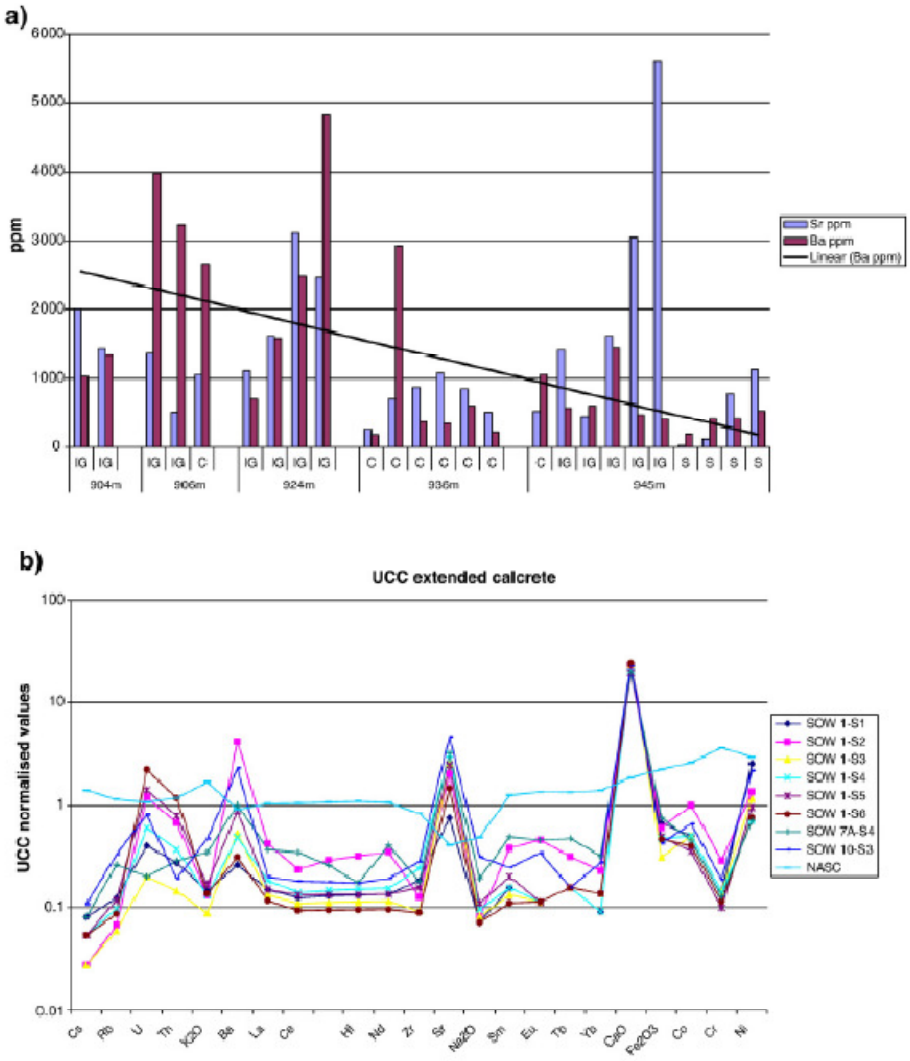

Fig. 5. a. Distribution Sr and Ba abundances across the main duricrust types differentiated by strandline elevation and duricrust type (C = calcrete, IG = silcrete–calcrete intergrade deposits, S = silcrete). b. Spider diagram showing normalized extended element anomalies relative to the NASC for calcretes in the PMSB, using normalizing values of Taylor and McClennan (1985).

and higher in the intergrade deposits (2–23 ppm). (Table 3) One anomalously high Th value occurs in the calcrete in the 906 m strandline (SOW10-S3., Fig. 7b) where values >20 ppm obtain in related calcretes and intergrade deposits. W concentrations range from 15 to 109 ppm throughout the duricrusts with particularly high concentrations in silcretes from the 945 m strandline (e.g. SOW7A-S1) and intergrades from the 906 m strandline (Table 3). The concentration levels for W are 2–50 times higher than the NASC levels for tungsten (Gromet et al., 1984). Yttrium abundances peak in intergrade sample SOW8A at 12 ppm whereas concentrations in calcrete and silcrete duricrusts are low at <8.5 ppm.

F abundances are relatively high in all the PMSB duricrusts with concentrations ranging from 200 to 860 ppm in the calcretes. SOW1 calcretes show an increase in F concentration with depth (Table 3). Silcrete–calcrete intergrade samples show a similar F range (220–770 ppm) with higher values coming from the 924 m deposit, SOW3-S2. The range for silcrete samples (160–790 ppm) indicates a high degree of overlap with the other duricrusts. The highest F value (860 ppm) occurs in calcretes from the 936 m strandline (SOW7A-S3) while the second highest F value (790 ppm) occurs in silcretes from the 945 m strandline where it corresponds to high concentrations of Zr. Boron concentrations (<46 ppm) are generally low whereas Cl values are often below the detection limit of the ICP-MS (Table 3). The highest Cl value (13 000 ppm) occurs in a silcrete (SOW13-S2) which is 40 km north of the present day Pan margin (Fig. 3). The second highest Cl value comes from SOW8A, close to the Pan margin (Table 3, Fig. 3).

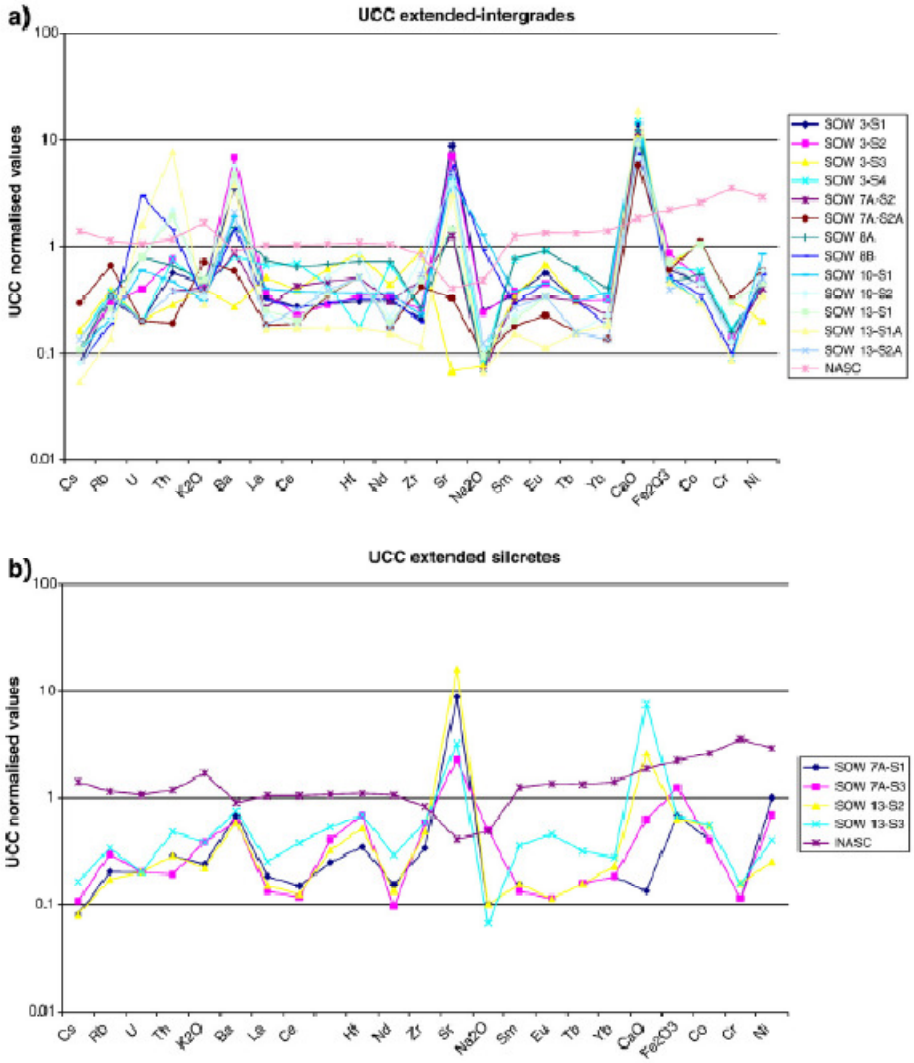

Fig. 6. a. Spider diagram showing normalized extended element anomalies relative to the NASC for intergrades in the PMSB, using normalizing values of Taylor and McClennan (1985). b. Spider diagram showing normalized extende d element anomalies relative to the NASC for silcretes in the PMSB, using normalizing values of Taylor and McClennan (1985).

4.4. High-field-strength-elements and REEs

In the PMSB duricrusts the Ta concentration is low (≤4.5 ppm) (Table 3). Niobium abundances are also low (~3 ppm) although higher values are found in the silcretes (at SOW7A S1) along the upper (945 m) strandlines (Fig. 3). Similarly low concentrations for Hf and Ga (at ~5 ppm) are generally prevalent (Fig. 7b). Near NASC values for Hf occur in both silcrete (SOW7A S1) and silcrete–calcrete intergrade deposits, (SOW10 S1). Here the Hf values are slightly lower than those found in the Karoo dolerites (Elburg and Goldberg, 2000). The highest Ga concentrations are found in the 945 m silcretes (e.g. SOW7A S3) although a Ga peak also occurs in SOW3 intergrade deposits (Fig. 7b). Very low HFSE concentrations occur in the calcretes.

Representative REEs (La, Ce and Nd) were initially plotted in histogram form (Fig. 8a) which shows an increase in La towards the lower strandlines. The REE content of the duricrusts is relatively low in the calcretes, high in the silcrete–calcrete intergrade deposits and intermediate in the silcretes (Table 4). The REE patterns were further normalized and re-plotted to show their relationship to the Upper Continental Crust. The transformations of Taylor and McLennan (1981) in relation to NASC normalized values were applied for each element (Gromet et al., 1984) over the REE range from La to Yb. Lu values were not used in this work as they were below the detection limits (Table 4). The UCC normalized results are plotted as Figs. 8b, 9a and b for the calcretes, intergrade deposits and silcretes, respectively. The UCC normalized patterns for calcretes and silcretes are much lower than the appropriate NASC lines, whereas intergrade duricrust normalized values are closer to the crustal shale average. Calcretes and silcrete–calcrete intergrade deposit patterns (Figs. 8b and 9a) are slightly convex upwards showing some MREE enrichment between La and Gd with

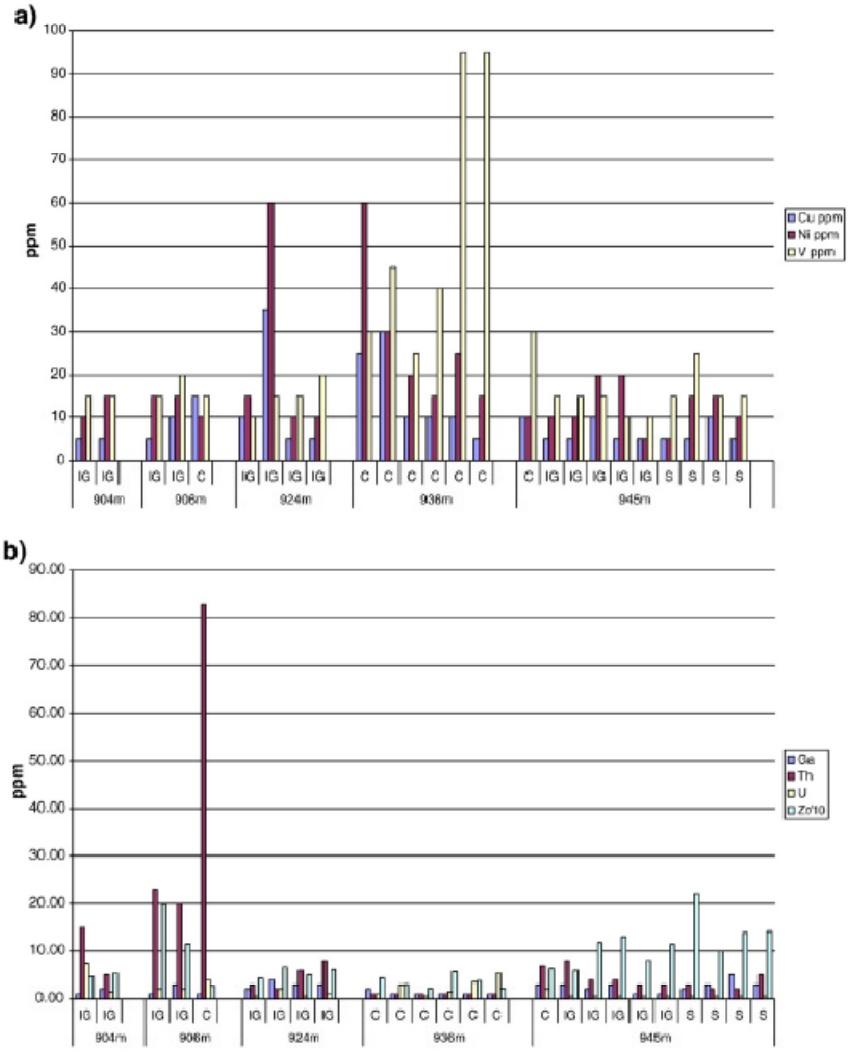

Fig. 7. a. Distribution of Cu, Ni and V abundances across the main duricrust types differentiated by strandline elevation and duricrust types (C = calcrete, IG = silcrete–calcrete intergrade deposits, S = silcrete). b. Distribution Zr, U, Th and Ya bundances across the main duricrust type s differentiated by strandline elevation and duricrust types (C = cal crete, IG = silcrete–calcrete intergrade deposits, S = silcrete).

variable HREE depletion between Gd and Yb. The patterns for silcretes show variable HREE enrichment between Gd and Yb (Fig. 9b). Ratios of Yb_n/Gd_n were therefore calculated to denote variations in HREE depletion or enrichment in the intergrade deposits and calcretes following procedures described in Elderfield et al. (1990). Values >1 signify enrichment while values <1 signify depletion (Fig. 10). Results show that most of the strandline duricrusts are relatively depleted in HREEs with some enrichment occurring in the 945 m silcretes, and single samples from the 936 m and 906 m strandline calcretes.

4.5. Stable isotopes

The $\delta^{13}C$ and $\delta^{18}O$ values of selected carbonate material from most strandlines range from −14.58 to +1.55‰ (mean −2.21‰) and 16.3 to 29.4‰ (mean 24.4‰), respectively (Table 5). Good positive correlation prevails between $\delta^{13}C$ and $\delta^{18}O$ values ($r = 0.94$) (Fig. 11a). In addition a strong positive correlation was found between both $\delta^{13}C$ and $\delta^{18}O$ and the wt.% calcite for those samples with <30% calcite which are mainly derived from the upper 945 m strandlines (Fig. 11b and c). This type of behaviour is characteristic of high temperature metamorphism of impure limestone (e.g. Valley, 1986), where loss of CO_2 lowers the $\delta^{13}C$ and $\delta^{18}O$ values of the remaining solid. However, CO_2 loss by decarbonation, is not possible in a low-temperature non-organic environment. One explanation for the correlation between $\delta^{13}C$ and $\delta^{18}O$ is that the carbonate did not form in isotope equilibrium with the fluids from which they precipitated and the correlations result from kinetic fractionation effects caused by the rapid loss of CO_2 from an aqueous fluid. Similar kinetic fractionation effects that produce correlations between $\delta^{13}C$ and $\delta^{18}O$ exist in some speleothems

Table 3
HFSE with U, Th, W and Y and halogen abundances in ppm from PMSB strandlines—SOW8A (904 m) to SOW7A (945 m).

Sample	Type	Ta	Nb	Ga	Hf	U	Th	W	Y	C	F	B	Cl
SOW8A	IG	0.5	<1	1.0	1.0	7.5	15.0	13.0	12.0	0.35	510.0	40.0	2710.0
SOW8B	IG	<0.5	<1	2.0	1.0	1.5	5.0	11.0	5.5	0.50	550.0	46.0	508.0
SOW10-S1	IG	1.0	1.0	1.0	5.0	2.0	23.0	23.0	7.0	0.50	300.0	22.0	77.0
SOW10-S2	IG	3.5	1.0	3.0	3.0	2.0	20.0	79.0	4.0	0.05	250.0	33.0	79.0
SOW10-S3	C	<0.5	<1	1.0	<1	4.0	83.0	9.0	4.5	0.30	200.0	8.0	<50
SOW3-S1	IG	0.5	1.0	2.0	1.0	0.5	3.0	16.0	6.5	0.20	550.0	<5	<50
SOW3-S2	IG	0.5	1.0	4.0	1.0	2.0	2.0	21.0	7.5	0.05	770.0	14.0	<50
SOW3-S3	IG	1.0	1.0	3.0	1.0	0.5	6.0	32.0	5.0	0.65	710.0	15.0	<60
SOW3-S4	IG	0.5	1.0	3.0	1.0	1.0	8.0	21.0	9.0	0.55	710.0	11.0	<50
SOW1-S1	C	<0.5	1.0	2.0	1.0	1.0	1.0	10.0	3.0	0.30	530.0	<5	<50
SOW1-S2	C	0.5	<1	1.0	<1	3.0	1.0	22.0	7.0	0.65	430.0	<5	<72
SOW1-S3	C	<0.5	<1	<1	<1	0.5	1.0	5.0	2.5	0.90	680.0	<5	<50
SOW1-S4	C	<0.5	<1	1.0	1.0	1.5	1.0	6.0	3.0	0.45	670.0	<5	<50
SOW1-S5	C	<0.5	<1	1.0	<1	3.5	1.0	4.0	2.5	0.65	860.0	<5	<50
SOW1-S6	C	<0.5	<1	1.0	<1	5.5	<1	7.0	2.5	0.30	340.0	<5	<60
SOW7A-S1	S	4.5	3.0	3.0	5.0	0.5	3.0	109.0	3.5	0.30	160.0	10.0	<50
SOW7A-S2	IG	1.5	1.0	3.0	1.0	0.5	8.0	37.0	6.5	0.15	650.0	12.0	<50
SOW7A-S2A	IG	0.5	1.0	2.0	3.0	0.5	4.0	23.0	3.0	0.25	660.0	16.0	<50
SOW7A-S3	S	3.0	3.0	5.0	3.0	0.5	2.0	77.0	2.5	0.10	790.0	29.0	<50
SOW7A-S4	C	<0.5	<1	3.0	1.0	2.0	7.0	12.0	8.5	0.45	440.0	17.0	<50
SOW13-S1	IG	0.5	1.0	3.0	3.0	0.5	4.0	23.0	4.0	0.55	650.0	16.0	97.0
SOW13-S1A	IG	<0.5	<1	1.0	2.0	0.5	3.0	6.0	3.0	1.30	630.0	10.0	130.0
SOW13-S2A	IG	0.5	1.0	1.0	3.0	0.5	3.0	23.0	4.0	0.90	220.0	9.0	140.0
SOW13-S2	S	0.5	1.0	2.0	4.0	0.5	2.0	15.0	2.5	0.35	430.0	17.0	13000.0
SOW13-S3	S	1.5	2.0	3.0	4.0	0.5	5.0	32.0	6.5	0.70	490.0	16.0	< 50

C = Calcrete, S = Silcrete, I/G = silcrete-calcrete intergrade deposit.

(Hendy, 1971) but further work is required to verify the exact process responsible here. In the discussions that follow, only data for samples with >30% calcite are used.

5. Discussion

5.1. Geochemical differences between the PMSB duricrusts

Trace element data from strandline duricrusts along the north-eastern margin of the Makgadikgadi Pans were evaluated to determine their contribution to the interpretation of complex calcrete, silcrete–calcrete intergrade and silcrete deposits. The main differences between the duricrust types have previously been described in terms of $SiO2/Al_2O_3$ and CaO rich end-members (Ringrose et al., 2005). The present trace element results are summarized as:

- The dominant alkali earths (Sr and Ba) show positive enrichment in the silcrete–calcrete intergrade deposits, intermediate values in the calcretes and low values in the silcretes (Figs. 5 and 6). Sr is high in the 945 m strandline with Ba dominant at the 906 m and 924 m levels.
- Whereas the lower calcretes have relatively high concentrations of V, Ni and U, most other trace elements (especially Zr, Th and HFSE) are more abundant in the intergrade deposits and to some extent in the silcretes (Fig. 7a and b).
- The silcrete–calcrete intergrade deposits have a relatively high REE content compared to the calcretes (Fig. 8a).
- Similarly, UCC normalized REE patterns for the calcretes depart more from that of the NASC continental crust than the silcrete–calcrete intergrade patterns, which show a closer affinity for the NASC continental crust (Figs. 8b and 9a).
- The REE patterns of calcretes and silcrete–calcrete intergrade deposits show a low MREE convexity (Figs. 8b and 9a) indicating HREE depletion (Fig. 10). Results from silcrete deposits are inconclusive.
- There is a generally positive correlation between $\delta^{13}C$ and $\delta^{18}O$, particularly in the intergrade deposits in the upper strandlines with <30% calcite (Fig. 11). There is a very strong positive correlation between wt.% calcite and $\delta^{13}C$ and $\delta^{18}O$ in those samples with <30% calcite which suggests non-equilibrium precipitation of calcite. As a consequence only samples with >30% calcite are used below to infer palaeo-climatic conditions.

5.2. Local and non-local bedrock sources relative to different duricrust types

The results show that differences occur in the trace element contents between the calcrete deposits and silcrete–calcrete intergrade deposits which given the replacive nature of the intergrade deposits, suggests different sources of porewater in each case. The background for these differences requires further consideration. The silica-rich duricrusts especially the silcrete–calcrete intergrade deposits contain more variable concentrations of major and trace elements and show closer resemblance to normalized continental crust profiles so the original porewater likely contained a higher proportion of dissolved or particulate weathered material when integrated over time. Weathering studies of rocks from the continental crust have shown that CaO, Na_2O, K_2O, Sr, Ba, Rb and U are the most soluble elements during chemical breakdown because of their high hydration energies (Nesbitt and Young 1982, 1984, 1989; Cullers 1988). Of these elements Sr, Ba, and Rb are more abundant in the silcrete–calcrete intergrade deposits whereas Na_2O, and K_2O are low throughout. This deficit may be attributed to the greater solubility of Na_2O, and K_2O confirming their selective removal during the weathering process and their deposition into the sub-pan groundwater (cf. Molwalefhe, 2003). Previous work on dolerite dyke composition around the pans (Elburg and Goldberg, 2000) and on the weathering of dolerite dykes from late Karoo sequences (Marsh, 1991) suggests that the weathering of *in situ* Karoo dolerites and basalts was accompanied by the progressive mobilization and removal of Si, Mg, Ca, Na, K, Rb, Sr, Ba, Y, and V into the PMSB regolith. We can therefore assume that once mobilized, these elements were available for groundwater transportation and were washed towards the then contemporary pan margin. Hence the chemical composition of the prevalent groundwater comprised a range of elements being strongly buffered by the composition of the bedrock and regolith (Kampunzu et al., 2007). This being so, a non-pedogenic origin is assumed for the duricrusts (cf. Wright and Tucker, 1991). The type of buffering envisaged is similar to

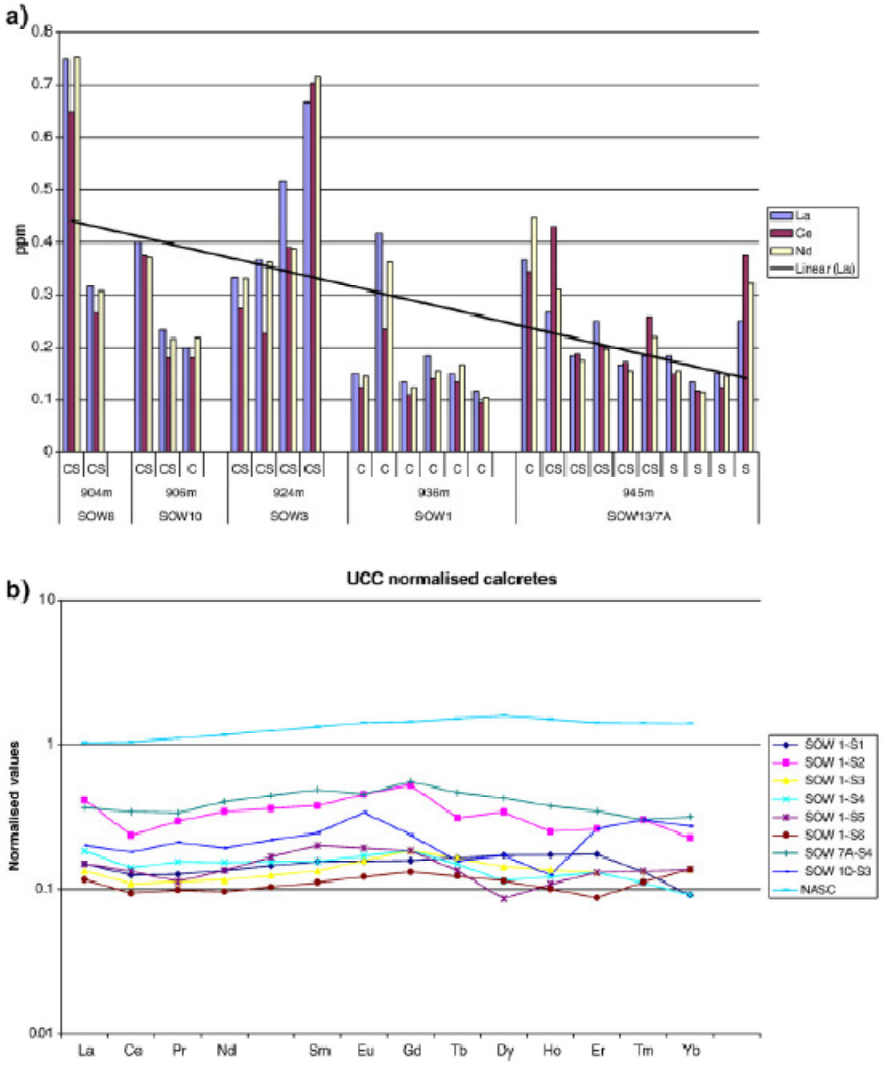

Fig. 8.. a. Distribution of selected REE abundances across the main duricrust types differentiated by strandline elevation and strandli. REE ppm: 0.1–0.2 = pH > 9, 0.3–0.4 = pH 7, >0.7 = pH5 (indicative pH values based on Dupreet al., 1996) (C = calcrete, IG = silcrete–calcrete intergrade deposits, S = silcrete). b. Upper continental crust normalized rare earth element distributions relative to the NASC for calcretes in the PMSB using normalizing values from Taylor and McClennan (1981) and Gromet et al. (1984).

that reported in southern Nevada where a strong correlation occurred between the major and trace element compositions of felsic and carbonate rocks and their respective local groundwater aquifers and aquitards (Stetzenbach et al., 2001). So the chemical composition of groundwaters leading to both calcretisation and silcretisation events can be viewed broadly in terms of chemical equilibria between weathered constituents and groundwater within the local aquifers (cf. Drever, 1997).

As the silica-enriched deposits contain a greater diversity and abundance of trace elements and result from secondary deposition into the calcrete then a more direct, localized source of groundwater flow through the contemporary weathering profile is envisaged. The calcrete deposits (hence the ground/porewaters leading to calcrete precipitation) comprise lower proportions and different trace elements suggesting that the source of Ca-enriched porewater differs from that of the Si-enriched porewater. Wang et al. (1994) suggested a model for calcrete genesis in which the main process was the introduction of large (exogenous) amounts of $CaCO_3$ through ground and surface water. This may be the case in the PMSB even though the weathering of overlying basalts and dolerites provides a Ca^{2+} source. If the high positive CaO anomalies (Figs. 5b and 6) suggest a need for Ca^{2+} importation from outside the immediate PMSB, then a non-localised source needs to be invoked (cf. Thomas and Shaw, 1991) and the Ca^{2+} is of mixed origin. Significant importation over time implies that the Ca^{2+} could be concentrated within the regional catchment (Fig. 4). The Okavango river catchment for instance includes

Table 4
Rare earth element abundances in ppm from PMSB strandlines–SOW8A (904 m) to SOW7A (945 m).

Sample	Type	La	Ce	Pr	Nd	Sm	Eu	Gd	Tb	Dy	Ho	Er	Tm	Yb	Lu
SOW8A	I/G	22.5	41.5	5.1	19.0	3.5	0.8	3.6	0.4	2.5	0.5	1.4	0.20	0.9	0.1
SOW8B	I/G	9.5	17.0	2.0	8.5	1.3	0.4	1.6	0.2	1.1	0.1	0.6	<0.1	0.4	<0.1
SOW10-S1	I/G	12.0	24.0	2.6	9.5	1.7	0.4	1.7	0.2	1.2	0.2	0.8	<0.1	0.8	0.1
SOW10-S2	I/G	7.0	11.5	1.4	5.5	1.0	0.3	1.2	0.1	0.6	0.1	0.5	<0.1	0.5	<0.1
SOW10-S3	C	6.0	11.5	1.5	5.0	1.1	0.3	0.9	0.1	0.6	0.1	0.6	<0.1	0.6	0.1
SOW3-S1	I/G	10.0	17.5	2.1	8.0	1.6	0.5	1.9	0.2	1.3	0.2	0.7	<0.1	0.7	<0.1
SOW3-S2	I/G	11.0	14.5	2.4	9.0	1.7	0.4	1.7	0.2	1.3	0.3	0.7	<0.1	0.7	0.1
SOW3-S3	I/G	15.5	25.0	3.5	11.5	1.5	0.6	1.9	0.2	1.1	0.2	0.6	<0.1	0.5	<0.1
SOW3-S4	I/G	20.0	45.0	4.8	17.5	3.4	0.8	2.6	0.4	1.8	0.3	1.0	0.10	0.7	0.1
SOW1-S1	C	4.5	8.0	0.9	3.5	0.7	0.1	0.6	<0.1	0.6	0.1	0.4	<0.1	0.2	<0.1
SOW1-S2	C	12.5	15.0	2.1	9.0	1.7	0.4	2.0	0.2	1.2	0.2	0.6	<0.1	0.5	<0.1
SOW1-S3	C	4.0	7.0	0.8	3.0	0.6	0.1	0.7	<0.1	0.5	<0.1	0.3	<0.1	0.3	<0.1
SOW1-S4	C	5.5	9.0	1.1	4.0	0.7	0.1	0.7	0.1	0.4	<0.1	0.3	<0.1	0.2	<0.1
SOW1-S5	C	4.5	8.5	0.8	3.5	0.9	0.1	0.7	<0.1	0.3	0.1	0.3	<0.1	0.3	<0.1
SOW1-S6	C	3.5	6.0	0.7	2.5	0.5	0.1	0.5	<0.1	0.4	<0.1	0.2	<0.1	0.3	<0.1
SOW7A-S 1	S	5.5	9.5	1.1	4.0	0.7	0.1	0.7	0.1	0.6	0.1	0.5	<0.1	0.4	<0.1
SOW7A-S 2	I/G	8.0	27.5	1.9	8.0	1.4	0.3	1.6	0.2	1.2	0.2	0.6	<0.1	0.5	0.1
SOW7A-S 2A	I/G	5.5	12.0	1.3	4.5	0.8	0.2	0.8	0.1	0.7	0.1	0.4	<0.1	0.3	<0.1
SOW7A-S 3	S	4.0	7.5	0.8	2.5	0.6	0.1	0.6	<0.1	0.4	0.1	0.3	<0.1	0.4	<0.1
SOW7A-S 4	C	11.0	22.0	2.4	10.5	2.2	0.4	2.1	0.3	1.5	0.3	0.8	0.10	0.7	0.1
SOW13-S1	I/G	7.5	13.0	1.5	5.0	0.9	0.3	1.0	0.1	0.8	0.1	0.5	<0.1	0.4	<0.1
SOW13-S1A	I/G	5.0	11.0	1.1	4.0	0.7	0.1	0.9	0.1	0.7	0.1	0.4	<0.1	0.4	<0.1
SOW13-S2A	I/G	5.5	16.5	1.2	4.5	1.2	0.3	1.0	0.1	0.7	0.1	0.4	<0.1	0.3	<0.1
SOW13-S2	S	4.5	8.0	1.1	3.5	0.7	0.1	0.8	<0.1	0.5	<0.1	0.3	<0.1	0.5	<0.1
SOW13-S3	S	7.5	24.0	1.7	7.5	1.6	0.4	1.7	0.2	1.3	0.2	0.7	<0.1	0.6	<0.1

C = Calcrete, S = Silcrete, I/G = silcrete–calcrete intergrade deposit.

extensive, open water bodies perennially undergoing evaporation/evapo-transpiration leading to relative Ca^{2+} enrichment (Wolski and Savenije; 2006; Ringrose et al., 2008). If a geochemical similarity is assumed over time, then inflow water with a relatively high Ca^{2+} concentration (McCarthy and Ellery, 1995; Cronberg, 1996) could flow into the PMSB through surface water sources (such as the Boteti river, Fig. 3) over extended geological time scales. An additional line of evidence implying long-range sources over time stems from work by Union Carbide (1980) who reported on uranium prospecting in the palaeo-drainage valleys which flow into the Okavango river system and hence the PMSB. The affinity of carbonates for U has been well documented (Carlisle, 1983; Mann and Deutscher, 1978). As there are no known U sources in the vicinity of the PMSB, the U in the strandline samples may have been derived from palaeo-Okavango river flow. This would be added to the Ca^{2+} contributed through the weathering of the Karoo Large Igneous Province rocks since the end of the Jurassic (e.g. Du Plessis, 1993). However this may be complemented as for instance in work by Semenunik and Meagher (1981) and Tandon and Kumar (1999) who indicate that the composition of calcretes mainly reflects groundwater composition and hence the weathering environment, from which they were derived. The local groundwater source is augmented by the notable presence of Cu and Ni in the 936 m (and adjacent 924 m) strandlines, in this case suggesting a local origin. The closest known location for these elements is the nearby Dukwe sulphide mine (Fig. 2) which is upstream of the 924 m and 936 m duricrusts. So the Ca^{2+} in the calcretes in the 924 m and 936 m strandlines for instance, appears to have been derived from both distant (regional) sources (which also contributed the U) and local sources which also contributed the Cu and Ni. Hence the concentration of $CaCO_3$ at the pan margins resulted from the mixing of exogenous Ca^{2+} from the catchment with endogenous weathered Ca^{2+} from groundwater flow. Catchment waters flowed through the incoming streams which during high rainfall events accumulated in the then contemporary pan-like depression and infiltrated into the pan-marginal sands where mixing occurred with the local groundwater. The repeated collection of water in the pan-like depression from regional and local rainfall events likely contributed to its deepening over time and has implications for the origin of the Makgadikgadi Pans which is beyond the scope of the present work. What is suggested here is that an explanation for the difference between Ca^{2+} enriched groundwater and Si-enriched groundwater appears dependent on the nature of inflow events. Results from trace element identification suggest that the abundant Ca^{2+} is derived from both local and regional sources while the Si is more locally derived. Different palaeo-climatic conditions may be invoked to explain these differences.

5.3. Duricrust origins and palaeo-climatic interpretations

As the incoming silica-rich groundwater with a relatively high concentration of trace elements most feasibly originated directly from localized groundwater flow, this seems to imply localized seasonal, rainfall. This contrasts with the Ca-rich water which is considered to have been derived from both local groundwater and externally derived surface sources. On the basis of $CaCO_3$ abundance in the basin, this implies heavier catchment-wide rainfall which would facilitate widespread Ca^{2+} uptake and re-distribution. The surface flow and groundwaters are thought to collect in a pan-like depression where the calcrete preferentially precipitates at the pan margin during a subsequent drying phase. Calcrete precipitation taking place on the edge of a pan, following temporary infilling and evaporation is consistent with the Eugster and Kelts (1983) evaporative sequence. Surface waters in the pan-like depression would have the effect of diluting both major and trace element inflow thereby explaining the lower trace element concentrations in the calcretes from both sources. Similarly the repeated infilling and drying episodes could help explain the multiple calcretisation events and the sequence of younger and older ages for a given strandline (Table 1). As the silica-rich groundwaters are mostly locally derived from groundwater sources, then their concentration at the pan margin in the calcrete strandlines requires further explanation. The prevalence of precipitated silica along the pan margins is evident from field observations at the present time where both ground and surface (rain) water collect in pan-marginal pools (F). The pools are found wherever the pan surface dips and therefore loci for pools in the past could well have been adjacent to the peripheral calcrete mounds. Summerfield (1983a) noted increasing concentrations of silica in rivers flowing into the Makgadikgadi Pans from which silcrete has directly precipitated. Since the pans are a closed surface/groundwater basin local inflow and groundwaters concentrate silica above the equilibrium solubility for quartz (cf. Thomas and Shaw, 1991) and hence tend to collect trace

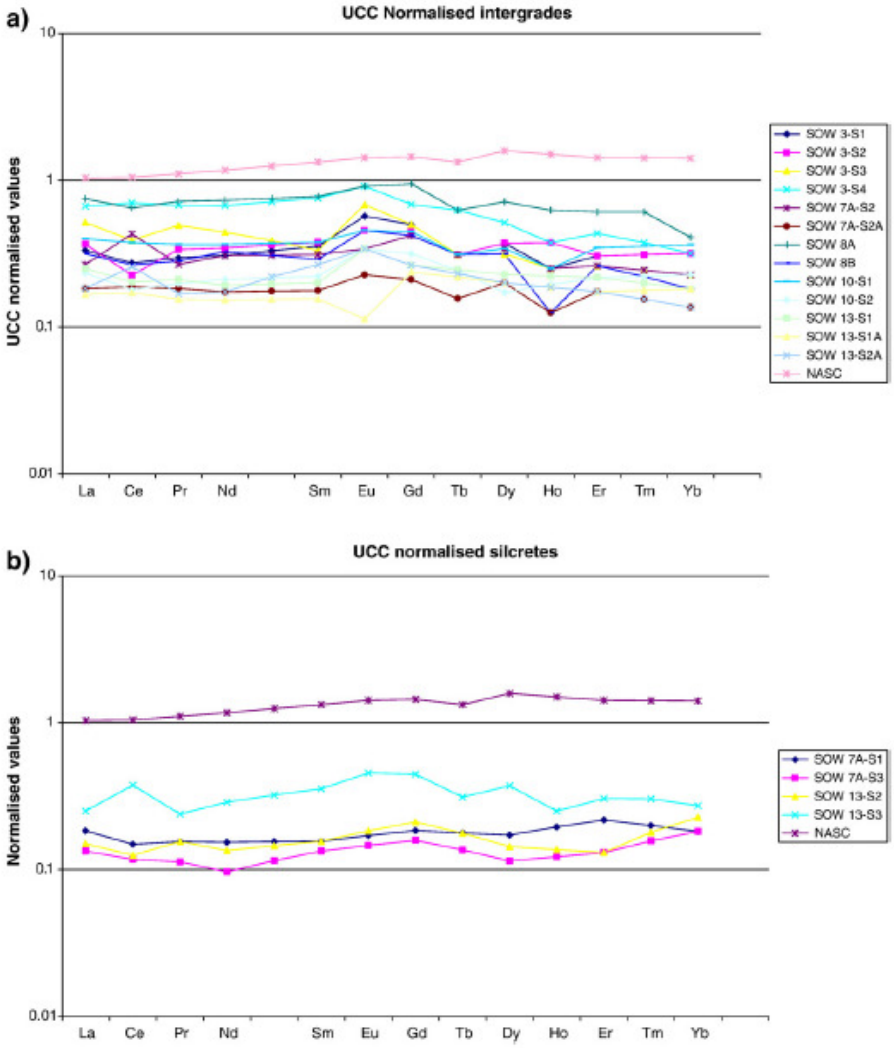

Fig. 9. a. Upper continental crust normalized rare earth element distributions relative to the NASC for intergrades in the PMSB using normalizing values from Taylor and McClennan (1981) and Gromet et al. (1984). b. Upper continental crust normalized rare earth element distributions relative to the NASC for silcretes in the PMSB, using normalizing values from Taylor and McClennan (1981) and Gromet et al. (1984).

elements. Inferred palaeo-climates needed for much of the silcretisation could therefore result from climatic conditions similar to those occurring today which comprise localised rainfall with minimal stream inputs into pan-marginal pools. Interestingly the silica does not precipitate upon evaporation but rather as the pH lowers towards near neutral (e.g. Nash and Shaw, 1998). Explanations for the lowering of the pH are normally ascribed to additional inputs of fresh water from the subsequent wet season. Hence silcrete precipitation or silica-rich incursions into pre-existing calcrete required repeated wet–dry seasonal cycles, similar to those occurring in Botswana at the present time. For clarity the very wet, catchment-wide humid phases required for calcrete formation are referred to as humid intervals and are followed by drying events required to effect calcretisation (Table 1). In this context silcretisation events are seen as secondary, taking place when climatic conditions reverted to more 'normal' semi-arid seasonally wet–dry cycles.

While silica-rich lithoclasts in the silcrete–calcrete intergrade deposits contain a suite of weathered minerals, the anomalously high Sr and Ba content (Figs. 5 and 6) requires further explanation. As the element concentrations differ over the different strandline elevations (Fig. 5a) this suggests the possibility of fractionation effects leading to the release of initially more Sr and then more Ba within the weathering sequence. A further possibility is that the relatively high Sr (and maybe Ba) abundances are biologically sequestered. In Lake Constance (Switzerland) high Sr/Ca ratios (in the freshwater lake) occur as the Sr is biologically mediated through algae in a process that leads to co-precipitation with sinking particulate organic matter (Stabel, 1989). Other literature sources indicate that lake plants may either favour Ca uptake over Sr or the converse depending on the plant in question, for instance in Perch Lake, Ontario (Ophel and Fraser, 1970). A biological uptake mechanism may be invoked where this

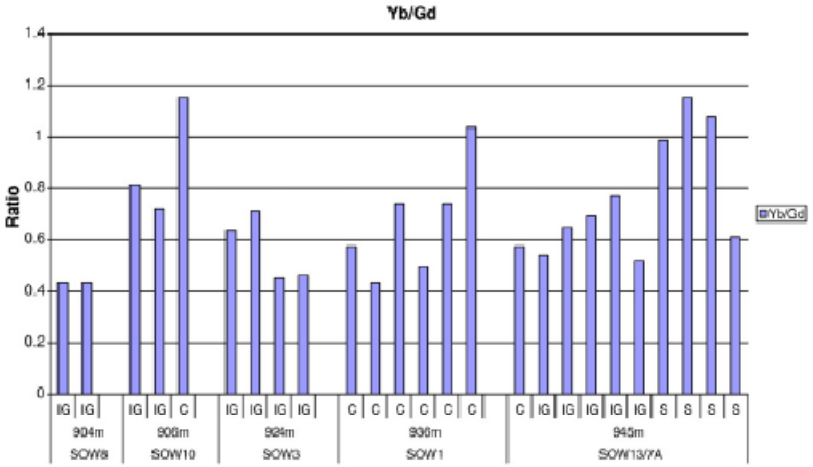

Fig. 10. HREE enrichment/depletion (Yb_n/La_n) ratios (after Elderfield et al., 1990) across the main duricrust types differentiated by strandline elevation (C = calcrete, IG = silcrete–calcrete intergrade deposits, S = silcrete).

occurs along the pan margin in the presence of abundant (and maybe varied) plant life. Assuming that small fresh water pools developed along the pan margin then plant action may have preferentially favoured the uptake of Sr (and maybe Ba) during different ponding phases over time. The Sr, Ba (and Si) formed part of the plant cells which were later entombed within silcrete–calcrete intergrade deposits, although other forms of biogenic concentration (e.g. through diatoms) are also possible. Some pan-marginal silcrete–calcrete intergrade deposits (from SOW2, 3 and 4) are associated with remnant plant (root) materials in the form of silica-rich rhizoliths (Table 1 and Ringrose et al., 2005). The silicification of plant remnants may have been initiated in macrophytes in a similar way to the plant uptake of Si as phytoliths in the Okavango Delta at present (cf. Struyf et al., 2007 in tidal environments). Silica-enriched rhizoliths occur especially in the 906 and 924 m strandlines which are noted for their high Ba concentrations, while anomalously high Sr concentrations are particularly found in the higher (945 m) strandlines which are not characterized by plant remains and therefore may have been sequestered through a different medium. Overall, the different relative abundances of transition metals may signify a change in geochemical environment but a full biological explanation as to why this has taken place (from the 945 m to the 904 m strandlines) is beyond the scope of the present work.

While the fact of silica concentration around the pan margins is undisputed, evidence suggesting fresh or slightly brackish marginal pan water contradicts consideration of the pan margin being highly saline and alkaline (e.g. Vink and Ringrose, 2001). The concentration of silica above the equilibrium level in the strandlines may be related to highly saline–alkaline marginal pan water (Williams and Crerar, 1984) and may be biogenically induced (Shaw et al., 1990). However the precipitation of silica has been described in Nash and Shaw (1998) as resulting from inputs of fresh water (mainly rainfall) which lowers the pH and thereby induces silica precipitation. So whereas the silica may concentrate under highly alkaline–saline conditions it appears to precipitate in a lower pH environment. The geochemical conditions under which precipitation took place may be further informed by the analysis of REE results.

5.4. Analysis and interpretation of REE results

Further insight into the geochemical environment prevalent along the pan margin during the formation of strandline duricrusts is suggested by dissolved REE concentrations. In natural waters these display an inverse correlation with pH values (Keasler and Loveland, 1982; Goldstein and Jacobsen, 1988; Elderfield et al., 1990; Sholkovitz, 1995) and this correlation is stronger (i.e. lowest REE concentrations occur) at pH > 6.5 (e.g., Dupré et al., 1996; Kampunzu et al., 2007). The REE results (Fig. 8a) when compared to relationships shown in Dupré et al. (1996), suggest that calcrete precipitation in the 936 m strandline took place over a range of pH values from pH 7 to pH 9. While this is approximate and bearing in mind that the Dupré et al. (1996) examples are for Congo river water, this mainly confirms that calcrete precipitation took place in a basic (bicarbonate-rich) environment which was therefore alkaline but not necessarily saline. This is turn supports suggestions that $CaCO_3$ precipitation took place after the pan margins were relatively wet and therefore likely following infilling from both surface and groundwater flow.

Higher REE concentrations were found in the silcrete–calcrete intergrade profiles for instance in the 924 m and 904 m strandlines which could infer porewater conditions which ranged from ≈pH 5 to pH 7. This suggests that at these locations, the silica-rich porewaters precipitated (in the pre-existing calcretes) under lower pH (near-neutral-acidic) conditions. At the 945 m and 906 m locations more

Table 5
C- and O-isotope composition of selected PMSB duricrust samples.

Sample	%c	$\delta^{13}C$ PDB	$\delta^{18}O$ SMOW	t °C − 4‰	t °C − 5‰	t °C − 6‰
SOW1-S1	86	−1.78	24.8	24	20	15
SOW1-S2	83	−3.45	25.2	23	18	14
SOW1-S3	85	1.45	26.9	16	11	7
SOW1-S4	82	−0.88	25.5	22	17	13
SOW1-S5	78	−0.77	25.6	21	17	12
SOW1-S6	41	−1.29	25.3	22	18	13
SOW10-S3	56	1.55	27.3	14	10	6
SOW3-S1	72	1.49	25.6	21	17	12
SOW3-S3	4	−8.97	18.3	60	54	48
SOW7A-S2	14	−2.02	23.5	31	26	21
SOW8A	28	2.45	29.4	5	1	−2
SOW10-S1	81	−0.59	27.5	13	9	5
SOW13-S1A	15	−1.51	24.5	26	21	17
SOW13-S2A	6	−5.80	19.4	53	47	42
SOW7A-S4	31	−0.69	26.2	18	14	10
SOW3-S4	1	−14.58	16.3	74	67	60

Notes: The % calcite was calculated from the yield of CO_2 during carbonate reaction at 25 °C. Temperatures of formation are calculated assuming equilibrium with water having $\delta^{18}O$ values of −4, −5 and −6‰.

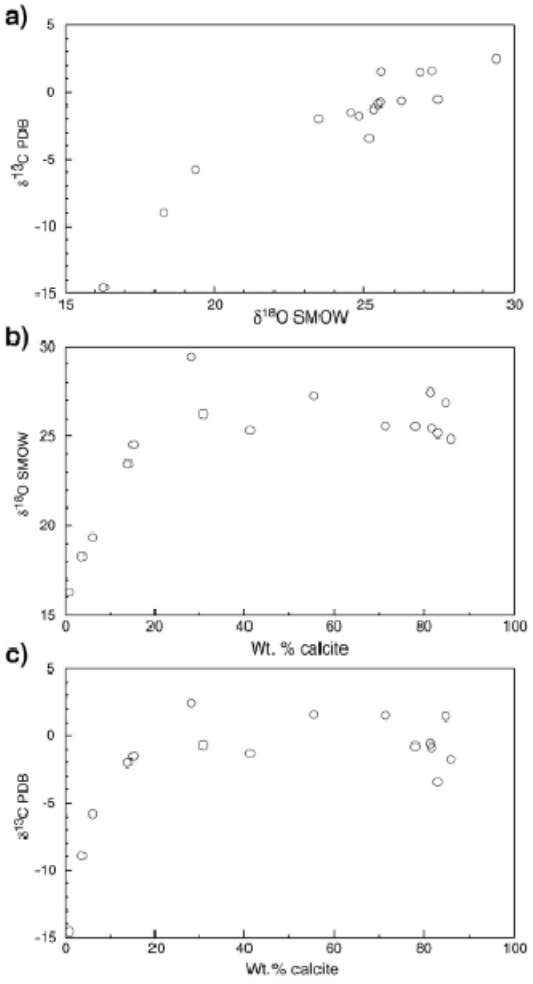

Fig. 11. (a) Plot of $\delta^{13}C$ relative to PDB vs $\delta^{18}O$ relative to SMOW for PMSB duricrusts, (b) $\delta^{18}O$ vs the wt% calcite and (c) $\delta^{13}C$ vs wt.% calcite, determined during carbonate extraction for isotope analysis.

mixed conditions prevailed but these average around pH 7–8 suggesting that porewater conditions were near neutral to slightly basic. The low pH range for silcretisation events supports the suggestion in Nash and Shaw (1998) that precipitation occurs when fresher waters are added to the pan-marginal pools. This is turn agrees with suggestions above that silcretisation involves the concentration of silica (and trace element) enriched waters near the pan margin but that the precipitation of silica likely occurred during the next seasons (low) rainfall as inputs of fresh water are required to lower the pH.

Evidence from REE patterns is further invoked to suggest whether the porewaters were saline during the processes leading to precipitation or whether this took place from essentially fresh water. Duricrust REE patterns (Fig. 8b, 9a and b) can be interpreted to infer the mixing of saline and fresher water sources. The stability of REE carbonate complexes increases with the atomic number and this favours a preferential retention of HREE compared to LREE (Sholkovitz, 1995). Details of estuarine mixing in terms of HREE depletion are described in Elderfield et al. (1990) whereby the flocculation of heavier elements corresponds to the onset of salinity. Non-normalized HREE enrichment ($Yb_n/Gd_n > 1$) or depletion ($Yb_n/Gd_n < 1$), where depletion corresponds to the onset of flocculation, can be used to infer the degree of mixing in terms of saline–freshwater conditions (Fig. 10). The silcrete–calcrete intergrade patterns show HREE depletion from the 904 m strandline denoted by Yb_n/Gd_n ratios of 0.43 inferring that saline conditions prevailed close to the present day pan margin and hence higher salinities are associated with the Holocene intergrade duricrusts (cf. Vink and Ringrose, 2001) (Table 1). However other (Pre-Holocene) intergrade deposit patterns are less determinate. For instance the 906 m strandline has high Yb_n/Gd_n ratios (1.15) in the calcretes inferring enrichment and so probable freshwater conditions while the relatively depleted intergrade deposits (at ≈0.75) suggests some flocculation and the onset of salinity, hence more brackish conditions. Results from the 924 m strandline depict a range of Yb_n/Gd_n values between 0.48 and 0.7 again suggesting a range of conditions varying from saline to brackish. The silcrete ratios range from 0.6 to 1.1 suggesting that they formed from mostly fresh porewaters. The Yb_n/Gd_n values of the silcrete–calcrete intergrade deposits suggest that the salinity of the pan margin pools varied from saline to brackish to fresh which might suggest a range of conditions (cf. Lee, 2006). Hence the result of the Yb_n/Gd_n ratio for predicting palaeo-climates relative to silcretisation events is inconclusive.

The calcrete Yb_n/Gd_n ratios (Fig. 10) from the 936 m strandline range between 0.4 and 1.0 suggesting that the calcretes formed from saline to fresh porewaters which as indicated above, were also alkaline. The 906 m strandline calcretes also appear to have precipitated from non-saline waters while the 945 m calcretes appear to have precipitated from saline waters. This might suggest that salinity has no bearing on calcrete precipitation which is mainly controlled by the pH and therefore again the Yb_n/Gd_n ratio is not particularly helpful.

However the balance of the evidence suggests that the ubiquitous precursor calcrete strandlines result from a highly evaporative Ca-enriched palaeo-environment whose origins infer extensive regional rainfall and extensive water collection thereby inferring major humid conditions. The subsequent silcretisation events infer lesser, more localized rainfall and more discrete pan-marginal ponding often alongside the pre-existing calcretes taking place under similar semi-arid conditions to those occurring at present. However conditions in the bicarbonate-rich pan waters which led to the deposition of calcretes at the 936 m strandline were unique being inimical to subsequent silcretisation. Why this calcrete did not transform into a more 'normal' intergrade deposit as a result of wet–dry cycles is further explained by isotope results.

5.5. Contribution of isotope data to understanding calcrete formation

The C- and O-isotope composition of the PMSB calcretes at the 936 m level was compared to calcretes from other locations worldwide (Fig. 12). The $\delta^{18}O$ values plot in the middle of the range of values for other calcretes, whereas the $\delta^{13}C$ values are relatively high but compare with values from the Gangetic Plains and the Thar Desert (NW India) which are both arid areas. Cerling (1991) shows that pure C3 and C4 plants produce $\delta^{13}C$ and $\delta^{18}O$ values of −12‰ and +2‰, respectively (cf. Quade et al., 1995). Thus a mixture of 50% C3 and 50% C4 plant contributions to the calcrete would have produced a $\delta^{13}C$ value of about −5‰. This suggests that the PMSB vegetation during the formation of the 936 m strandline calcretes comprised a mixture of grass and shrubs similar to that which occurs at present.

The $\delta^{18}O$ value of calcrete carbonate depends on the $\delta^{18}O$ value of the porewater from which the calcite precipitated and the temperature of formation. The expected $\delta^{18}O$ value of ambient rainwater in the area is unknown but present day data for Pretoria, Windhoek and Harare are available from the IAEA data base (Rozanski et al., 1993) for the years 1961–1987. The weighted mean $\delta^{18}O$ values for these locations are

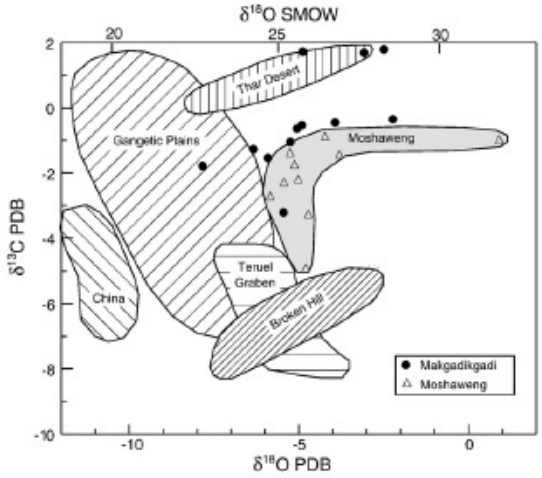

Fig. 12. Plot of $\delta^{13}C$ vs $\delta^{18}O$ for PMSB calcretes (>30 wt.% calcite) in comparison to global isotope results. Fields for the Gangetic Plains are taken from Srivastava (2001), the Thar Desert NW India (Andrews et al., 1998), loess fields of China (Rowe and Maher, 2000), the Teruel Graben, Central Spain (Alonso-Zarzaa and Arenas (2004) and Broken Hill, Australia (Schmid et al., 2006).

−3.7‰, −5.0‰, and −6.1‰, respectively. Hence the expected weighted mean $\delta^{18}O$ value of rainfall in area at the present day is probably between −4 and −6‰. Table 5 gives the temperature for calcite in equilibrium with water calculated using the equation $1000\ln\alpha_{calcite-water} = 2.78*(10^6/T^2) - 2.89$ (Friedman and O'Neill, 1977) for water having $\delta^{18}O$ values of −4, −5 and −6‰. The samples with the lowest % calcite (and hence low $\delta^{18}O$, Fig. 11) give unrealistically high temperatures for all three water $\delta^{18}O$ values and are ignored in the average temperature calculations that follow. The calcite in the samples with >30% calcite has an average $\delta^{18}O$ value of 26.29‰ and this gives temperatures of 17.9, 13.6 and 9.4 °C, for water $\delta^{18}O$ values of −4, −5 and −6‰, respectively. For the water $\delta^{18}O$ value of −4‰, the average temperature of 17.9 °C is close to the mean annual temperature of 18.8 °C (Gaborone, Botswana in Cooke, 1987). For a water $\delta^{18}O$ value of −6‰, the temperature of equilibration of the calcite in the calcrete is significantly lower with an average value of 9.4 °C, which is clearly below the present day mean annual average temperature. During a period of colder climate, the $\delta^{18}O$ of rainfall would be expected to be somewhat lower than the value observed today. This would lead to estimates of formation temperature of calcite that are even lower than in Table 5, and hence clearly unrealistic. Present day groundwater from Orapa in central Botswana has a $\delta^{18}O$ value of around −6‰ (Mazor et al., 1977) so it seems likely that there was significant groundwater evaporation during calcrete formation, which raised the $\delta^{18}O$ value. The amount of evaporation required to raise the $\delta^{18}O$ of water by a certain amount depends on the amount of water lost as vapor and humidity at the time of evaporation and is not simple to calculate. The lower $\delta^{18}O$ values of the PMSB samples compared to the Moshaweng (Kampunzu et al., 2007) samples suggest generally lower $\delta^{18}O$ values of the water from which they formed, or higher temperatures. Higher temperatures would normally go hand in hand with higher water $\delta^{18}O$ values of rainfall. It is much more likely that the cause of the lower $\delta^{18}O$ values in the PMSB calcretes reflects lower rainfall $\delta^{18}O$ values and hence lower annual temperatures than are present today (Table 5). Calcrete precipitation under low temperatures is evident from the literature as indicated in Strong et al. (1992). Hence while the Ca^{2+} forming the 936 m strandline might have formed at the pan margin following a heavier rainfall phase and the carbonates precipitated during a time of high evapo-transpiration, this appears to have taken place under much cooler conditions than those prevailing today. The cooler, drier conditions may have reduced the chances of localized rainfall and the development of pan-marginal pools thereby impeding silcretisation. Hence the wetter and drier cycles which characterize the evolution of the PMSB were interspersed by cooler, drier intervals defined by isotope results which in this case likely occurred > 80–90 000 years ago (Table 1).

6. Conclusions

Trace element data from PMSB strandline duricrusts were evaluated to help determine whether such data could help in their interpretation and thereby assist in elucidating palaeo-climatic conditions. On the basis of trace element content and relative abundance, it is suggested that the duricrust origins are associated with the long-term weathering of the Karoo Large Igneous Province which underlies the pans. Trace element data associated with calcrete deposition infers mixed local and regional sources whereas the trace elements associated with silcretisation events suggest a derivation solely from local groundwater. Local groundwater feeding in towards the pan margin and accumulating in pan-marginal pools, appear to have been repeated precursors for Si concentration. The later permeation of pre-existing calcretes (F) took place when the pH dropped after renewed rainfall. The need for seasonal wet–dry intervals suggests that a palaeo-climatic regime for silcretisation may be similar to that occurring in Botswana at present. In contrast the extensive $CaCO_3$ precipitation resulting from abundant Ca^{2+} in adjacent waters appears to be derived from both local and regional sources based on trace element data. The arrival of Ca^{2+} from regional sources suggests heavy rainfall in the upper catchment and therefore a major humid event. Hence general palaeo-climatic conditions infer the juxtaposition of major humid events interspersed with more normal semi-arid palaeo-climates over very long time scales. An exception obtained from isotope data suggests drier, colder conditions than usual for the region around 80–90 000 years ago. Whereas trace element data can greatly assist in the interpretation of complex deposits such as duricrusts, care should be taken over the use of particular ratios (such as Yb/Gd ratio) which may produce spurious results.

Acknowledgements

The authors would like to re-dedicate this work to Professor 'Henri' Kampunzu who passed away in November, 2004. The authors wish to thank Monica Morrison for referencing and editing assistance and to acknowledge financial assistance from the University of Botswana, Research and Publications Committee (Grant RPC 511). Sincere thanks are extended to Dr David Nash, Brighton University who provided very helpful comments on an early version of this work.

References

Alonso-Zarzaa, A.M., Arenas, C., 2004. Cenozoic calcretes from the Teruel Graben, Spain: microstructure, stable isotope geochemistry and environmental significance. Sediment. Geol. 167, 91–108.
Amundson, R.G., Wang, Y., Chadwick, O.A., Trumbore, S.L., McFadden, McDonald, E., Wells, S., De Niro, M., 1994. Factors and processes governing the 14C content of carbonate in desert soils. Earth Planet. Sci. Lett. 125, 385–405.
Andrews, J.E., Singhvi, A.K., Kailath, A.J., Kuhn, R., Dennis, P.F., Tandon, S.K., Dhir, R.P., 1998. Do stable isotope data from calcrete record Late Pleistocene reflect monsoonal climate variation in the Thar Desert of India? Quat. Res. 50, 240–251.
Bhalotra, Y.P.R., 1987. Climate of Botswana, Part II: elements of climate, rainfall. Dept Met. Services, Ministry of Works and Communication, Gaborone, Botswana. 21pp.
Buck, B.J., Monger, H.C., 1999. Stable isotopes and soil-geomorphology as indicators of Holocene climate change, northern Chihuahuan Desert. J. Arid Environ. 43, 357–373.
Carlisle, D., 1983. Concentration of uranium and vanadium in calcretes and gypcretes. In: Wilson, R.C.L. (Ed.), Geol. Soc. London Special Publication, vol. 11, pp. 185–195.
Cooke, H.J., 1978. Botswana's present climate and the evidence for past change. Proceedings of the Symposium of Drought in Botswana, National Museum (Botswana Society), Gaborone, Botswana, pp. 53–58.

Cooke, H.J., Verstappen, H.Th., 1984. The landforms of the western Makgadikgadi basin in northern Botswana, with consideration of the chronology of the evolution of Lake Palaeo-Makgadikgadi. Zeit. Geomorph., N.F.Bd28, Heft, vol. 1, pp. 1–19.
Cronberg, G., Gieske, A., Martins, E., Prince-Nengu, J., Stenstrom, L-M., 1996. Major ion chemistry, plankton and bacterial assemblages of the Jao/Boro River, Okavango Delta, Botswana: the swamps and floodplains. Arch. Hydrobiol./Suppl. 107 (Monographic Studies) Stuttgart, vol. 3, pp. 335–407.
Cerling, T.E., 1991. Carbon dioxide in the atmosphere: evidence from Cenozoic and Mesozoic paleosols. Am. J. Sci. 291, 377–400.
Chilingar, G.V., 1963. Ca/Mg and Sr/Ca ratios of calcareous sediments as a function of depth and distance from shore. J. Sediment. Petrol. 33, 236–245.
Cullers, R.L., 1988. Mineralogical and chemical changes of soil and stream sediment formed by intense weathering of the Danberg granite, Georgia, USA. Lithos 21, 301–314.
Davies, M., Jenkins, G., 2003. Tarcoola calcrete geochemistry database. Mesa J. 31 (http://www.pir.sa.gov.au/__data/assets/pdf_file/0003/10965/mj31_tarcoola_calcrete.pdf).
Deutz, P., Montanez, I.P., Monger, H.C., Morrison, J., 2001. Morphology and isotope heterogeneity of late Quaternary pedogenic carbonates: implications for paleosol carbonates as paleoenvironmental proxies. Palaeogeog. Palaeoclim. Palaeoecol. 166, 293–317.
Drever, J.I., 1997. The Geochemistry of Natural Waters, Surface and Groundwater Environments, Third Ed. Prentice Hall, NJ. 436 pp.
Du Plessis, P.L., 1993. The sedimentology of the Kalahari Group in four study areas in northern Botswana, Unpublished MSc thesis, University of Stellenbosch, South Africa.
Dupré, B., Gaillardet, J., Rousseau, D., Allègre, C.J., 1996. Major and trace elements of river-borne material: the Congo Basin. Geochim. Cosmochim. Acta 60, 1301–1321.
Ellburg, M., Goldberg, A., 2000. Age and geochemistry of Karoo dolerite dykes from northeast Botswana. J. Afr. Earth Sci. 31, 539–554.
Elderfield, H., Upstill-Goddard, R., Sholkovitz, E.R., 1990. The rare earth element in rivers, estuaries, and coastal seas and their significance to the composition of ocean waters. Geochim. Cosmochim. Acta 54, 971–991.
Eugster, H.P., Kelts, K., 1983. Lacustrine chemical sediments. In: Goudie, A.G., Pye, K. (Eds.), Chemical Sediments and Geomorphology: Precipitates and Residua in the Near Surface Environment. InAcademic Press, London, pp. 321–368.
Fairbridge, R.V., 1964. The importance of limestone and its Ca/Mg content to palaeoclimatology. In: Nairn, A.E.M. (Ed.), Problems in Palaeoclimatology. InWiley, New York, pp. 431–530.
Friedman, I., O'Neill, J.R., 1977. Compilation of stable isotope fractionation factors of geochemical interest. U.S. Geol. Surv. Prof. Paper, 440-KK, pp. 1–12.
Geological Survey of Botswana, 2000. Geological map of the Republic of Botswana (digital edition). Geological Survey of Botswana, Lobatse, Botswana.
Goldstein, S.J., Jacobsen, S.B., 1988. Rare earth elements in river waters. Earth Planet. Sci. Lett. 89, 35–47.
Gould, D., 1986. Brines of Sowa Pan and adjacent areas, Botswana. Mineral Deposits of Southern Africa, I and II, pp. 2289–2299.
Gromet, L.P., Dymek, R.F., Haskin, L.A., Korotev, R.L., 1984. The "North American shale composite": its compilation, major and trace element characteristics. Geochim. Cosmochim. Acta 48, 2469–2482.
Hay, R.L., Reeder, R.J., 1978. Calcretes of Olduvai Gorge and Ndolonya beds of northern Tanzania. Sedimentology 25, 649–673.
Hendy, C.F., 1971. The isotopic geochemistry of speleothems—I, the calculation of the effects of different models of formation on the isotopic composition of speleothems and their applicability as palaeoclimatic indicators. Geochim. Cosmochim. Acta 35, 801–824.
Hoffmann, A.W., 1988. Chemical differentiation of the earth: the relationship between mantle, continental crust and oceanic crust. Earth Planet. Sci. Lett. 90, 297–314.
Huntsman-Mapila, P., Ringrose, S., Mackay, A.W., Downey, W.S., Modisi, M., Coetzee, S.H., Tiercelin, J.-J., Kampunzu, A.B., Vanderpost, C., 2006. Use of the geochemical and biological sedimentary record in establishing palaeo-environments and climate change in the Lake Ngami basin, NW Botswana. Quat. Int. 148, 51–64.
Jourdan, F., Feraud, G., Bertrand, H., Kampunzu, A.B., Tshoso, G., Le Gall, B., Tiercellin, J.-J., Capiez, P., 2004. The Karoo triple junction questioned: evidence from Jurassic and Proterozoic $^{40}Ar/^{39}Ar$ ages and geochemistry of the giant Okavango dyke swarm (Botswana). Earth Planet. Sci. Lett. 222, 989–1006.
Kampunzu, A.B., Ringrose, S., Huntsman-Mapila, P., Harris, C., Vink, B., 2007. Origins and palaeo-environments of Kalahari duricrusts in the Moshaweng dry valleys (Botswana, Kalahari) as detected by major and trace element composition. Afr. J. Earth Sci. 48, 199–221.
Kane, J.S., 1992. Reference samples for use in analytical geochemistry: their availability, preparation, and appropriate use. J. Geochem. Explor. 44, 37–63.
Keasler, K.M., Loveland, W.D., 1982. Rare earth elemental concentrations in some Pacific Northwest rivers. Earth Planet. Sci. Lett. 61, 68–72.
Lee, S., 2003. Groundwater geochemistry and associated hardpans in southwestern Australia. In: Roach, I.C. (Ed.), Advances in Regolith, CRC LEME. InCurtin University of Technology, Western Australia, pp. 254–258.
Mann, A.W., Deutscher, R.L., 1978. Genesis principles for the precipitation of carnotite in calcrete drainages. West. Aust. Econ. Geol. 73, 1724–1737.
Marsh, J.S., 1991. REE fractionation and Ce anomalies in weathered Karoo dolerite. Chem. Geol. 90, 189–194.
Mazor, E., Verhagen, B.T., Sellschop, J.P.F., Jones, M.T., Robins, N.E., Hutton, L., Jennings, C.M.H., 1977. Northern Kalahari groundwaters: hydrologic, isotopic and chemical studies at Orapa, Botswana. J. Hydrol. 34, 203–234.
McFarlane, M.J., Segadika, 2001. Archaeological evidence for the reassessment of the ages of the Makgadikgadi palaeolakes. Botsw. Notes Rec. 33, 83–92.
McRae, M., 1950. The isotopic chemistry of carbonates and a paleotemperature scale. J. Chem. Phys. 18, 849–857.
McCarthy, T.S., Ellery, W.N., 1995. Sedimentation on the distal reaches of the Okavango Fan, Botswana and its bearing on calcrete and silcrete (Ganister) formation. J. Sediment. Res. A65, 77–90.
Molwalefhe, L.N., 2003. Geochemical and isotopic characterization of shallow basinal brines from the Makgadikgadi Pans complex of Northeastern Botswana: determination of the source of salinity, Doctor of Philosophy thesis, University of Missouri Rolla, USA.
Monger, H.C., Cole, D.R., Gish, J.W., Giordano, T.H., 1998. Stable carbon and oxygen isotopes in Quaternary soil carbonates as indicators of ecogeomorphic changes in the northern Chihuahuan Desert, USA. Geoderma 82, 137–172.
Moore, A.E., Larkin, P., 2001. Drainage evolution in south-central Africa since the breakup of Gondwana. S. Afr. J. Geol. 104, 47–68.
Nash, D.J., Shaw, P.A., 1998. Silica and carbonate relationships in silcrete–calcrete intergrade duricrusts from the Kalahari desert of Botswana and Namibia. J. Afr. Earth Sci. 27, 11–25.
Nash, D.J., Thomas, D.S.G., Shaw, P.A., 1994. Siliceous duricrusts as palaeoclimatic indicators: evidence from the Kalahari desert of Botswana: Palaeogeog. Palaeoclim. Palaeoecol. 112, 279–295.
Nash, D.J., Mclaren, S.J., Webb, J.A., 2004. Petrology, geochemistry and environmental significance of silcrete–calcrete intergrade deposits at Kang Pan and Tswaane, central Kalahari, Botswana. Earth Surf. Processes Landf. 29, 1559–1585.
Nesbitt, H.W., Young, G.M., 1982. Early Proterozoic climates and plate motions inferred from major element chemistry of lutites. Nature 299, 715–717.
Nesbitt, H.W., Young, G.M., 1984. Prediction of some weathering trends of plutonic and volcanic rocks based on thermodynamic and kinetic considerations. Geochim. Cosmochim. Acta 1523–1534.
Nesbitt, H.W., Young, G.M., 1989. Formation and diagenesis of weathering profiles. J. Geol. 97, 129–149.
Ophel, I.L., Fraser, C.D., 1970. Calcium and strontium discrimination by aquatic plants. Ecology 51, 324–327.
Ødegard, M., 1997. Chemical analysis of rocks and soils. Ch 5 in Geochemical Processes. In: Saether, O.M., de Caritat, P. (Eds.), Weathering and Groundwater Recharge in Catchments, pp. 153–166.
Plank, T., Langmuir, C.H., 1998. The chemical composition of subducting sediment and its consequences for the crust and mantle. Chem. Geol. 145, 325–394.
Quade, J., Chivas, A.R., McCulloch, M.T., 1995. Strontium and carbon isotope tracers and the origins of soil carbonate in South Australia and Victoria. Palaeogeog. Palaeoclim. Palaeoecol. 113, 103–117.
Ringrose, S., Matheson, W., 2003. Assessment of vegetation cover trends and local ecological factors along the Botswana Kalahari Transect. J. Arid Environ. 54, 297–317.
Ringrose, S., Downey, B., Genecke, D., Sefe, F., Vink, B., 1999. Nature of sedimentary deposits in the western Makgadikgadi littoral zone. J. Arid Environ. 32, 281–299.
Ringrose, S., Kampunzu, A.B., Vink, B.W., Matheson, W., Downey, W.S., 2002. Origin and palaeo-environments of calcareous sediments in the Moshaweng dry valley, southeast Botswana. Earth Surf. Processes Landf. 27, 591–611.
Ringrose, S., Huntsman-Mapila, P., Kampunzu, H., Downey, W.D., Coetzee, S., Vink, B., Matheson, W., Vanderpost, C., 2005. Geomorphological and geochemical evidence for palaeo feature formation in the northern Makgadikgadi sub-basin, Botswana. Palaeogeog. Palaeoclim. Palaeoecol. 217, 265–287.
Ringrose, S., Huntsman-Mapila, P., Downey, W., Coetzee, S., Fey, M., Vanderpost, C., Vink, B., Kenosidile, T., Kolokose, D., 2008. Diagenesis in Okavango fan and adjacent dune deposits with implications for the record of palaeo-environmental change in Makgadikgadi–Okavango–Zambezi basin, northern Botswana. Geomorphology 101, 544–557.
Rowe, P.J., Maher, B.A., 2000. 'Cold' stage formation of calcrete nodules in the Chinese Loess Plateau: evidence from U-series dating and stable isotope analysis. Palaeogeog. Palaeoclim. Palaeoecol. 157, 109–125.
Rozanski, K., Araguas-Araguas, L., Gonfiantini, R., 1993. Isotopic patterns in Global Precipitation. Geophysical monograph 78, Amer. Geophysical Union, pp. 1–35.
Schmid, R., Worden, R.H., Fisher, Q.J., 2006. Variations of stable isotopes with depth in regolith calcite cements in the Broken Hill region, Australia: palaeoclimate evolution signal? J. Geochem. Explor. 89, 355–358.
Semeniuk, V., Meaghar, T.D., 1981. Calcrete in Quaternary coastal dunes in south western Australia: a capillary rise phenomenon associated with plants. J. Sediment. Petrol. 51, 47–68.
Shaw, P.A., Thomas, D.S.G., 1992. Geomorphological processes, environmental change and landscape sensitivity in the Kalahari region of southern Africa, 1992 In: Thomas, D.S.G., Allison, R. (Eds.), Landscape Sensitivity. InWiley, London, pp. 83–95.
Shaw, P.A., Cooke, H.J., Perry, C.C., 1990. Microbalitic silcretes in highly alkaline environments: some observations from Sua Pan, Botswana. S. Afr. J. Geol. 93, 803–808.
Sholkovitz, E.R., 1995. The aquatic chemistry of rare earth elements in rivers and estuaries. Aquat. Geochem. 1, 1–34.
Stabel, H.H., 1989. Coupling of strontium and calcium cycles in Lake Constance. Hydrobiologia 176/177, 323–329.
Stetzenbach, K.J., Hodge, V.F., Guo, C., Farnham, I.M., Johannesson, K.H., 2001. Geochemical and statistical evidence of deep carbonate groundwater within overlying volcanic rock aquifers/aquitards of Southern Nevada, USA. J. Hydrol. 243, 254–271.
Srivastava, P., 2001. Palaeoclimatic implications of pedogenic carbonates in Holocene soils of the Gangetic Plains, India. Palaeogeog. Palaeoclim. Palaeoecol. 172, 207–222.
Strong, G.E., Giles, J.R.A., Wright, V.P., 1992. A Holocene calcrete from North Yorkshire, England; implications for interpreting palaeoclimates using calcretes. Sedimentology 39, 333–347.
Struyf, E., Van Damme, S., Gribsholt, B., Bal, K., Beauchard, O., Middelburg, J.J., Meire, P., 2007. *Phragmites australis* and silica cycling in tidal wetlands. Aquat. Bot. doi:10.1016/j.aquabot.2007.05.002.
Summerfield, M.A., 1983a. Silcrete. In: Goudie, A.S., Pye, K. (Eds.), Chemical Sediments and Geomorphology. InLondon Academic Press, pp. 59–92.
Summerfield, M.A., 1983b. Silcrete as a palaeoclimatic indicator: evidence from southern Africa. Palaeogeog. Palaeoclim. Palaeoecol. 41, 65–79.

Tandon, S.K., Kumar, S., 1999. Semi-arid/arid zone calcretes: a review. In: Singhvi, A.K., Derbyshire, E. (Eds.), Palaeoenvironmental Reconstruction in Quaternary Arid Lands. InOxford and IBH Publishing Co., pp. 109–152.
Taylor, J.K., 1987. Quality Assurance of Chemical Measurements. Lewis Publishers, USA.
Taylor, S.R., McLennan, S.M., 1981. The composition and evolution of the continental crust: rare earth element evidence from sedimentary rocks. Phil. Trans. Roy. Soc. A301, 381–399.
Taylor, S.R., McLennan, S.M., 1985. The Continental Crust: Its Composition and Evolution. Blackwell Scientific, Oxford. 312 pp.
Thomas, D.S.G., Shaw, P.A., 1991. The Kalahari Environment. Cambridge University Press, Cambridge. 284 pp.
Thomas, D.S.G., Shaw, P.A., 2002. Late Quaternary environmental change in central southern Africa: new data, synthesis, issues and prospects. Quat. Sci. Rev. 21, 7.
Thompson, M., 1992. Data quality in applied geochemistry: the requirements and how to achieve them. J. Geochem. Explor. 44, 3–22.
Tiercelin, J.J., Lezzar, K.E., 2002. A 300 million year history of rift lakes in Central and east Africa: an updated broad review. In: Odada, E.O., Olago, D.O. (Eds.), The East African Great Lakes, Limnology, Palaeolimnology, and Biodiversity. InKluwer Academic Publishers, Dordrecht, pp. 3–60.
Union Carbide 1980 Final report on prospecting license numbers 26/78, 23/79, 6/79, 7/79, 8/79, 9/79, 4/79, 5/79, 3/80, 4/80 and 5/80 (D.J. Jack). Botswana Geological Survey Unpublished report CR28/2/9, Lobatse 17 pp + maps.
Valley, J.W., 1986. Stable isotope geochemistry of metamorphic rocks. Rev. Mineral. Geochem. 16, 445–489.
Vink, B., Ringrose, S., 2001. Occurrences of magadiite and kenyaite in calcrete samples from the Sowa pan, central Botswana. Botsw. J. Earth Sci. 5, 32–34.
Walker, T.R., 1960. Carbonate replacement of detrital crystalline silicate minerals as a source of authigenic minerals in sedimentary rocks. Bull. Geol. Soc. Am. 71, 145–152.
Wang, Y., Nahon, D., Merino, E., 1994. Dynamic model for the genesis of calcretes replacing silicate rocks in semi-arid regions. Geochim. Cosmochim. Acta 58, 5131–5145.
Williams, L.A., Crerar, D.A., 1984. Silica diagenesis II. General mechanisms. J. Sediment. Petrol. 55, 312–321.
Wright, V.P., Tucker, M.E. (Eds.), 1991. Calcretes, Reprint Series Volume 2 of the International Association of Sedimentologists. InBlackwell Scientific Publications Publishers, London.
Wolf, K.H., Chilingar, G.V., Beales, F.W., 1967. Elemental composition of carbonate skeletons, minerals and sediments. In: Chilingar, G.V., Bissell, H.J., Fairbridge, R. (Eds.), Carbonate Rocks, Physical and Chemical Aspects, pp. 23–150.
Wolski, P., Savenije, H.H.G., 2006. Dynamics of floodplain-island groundwater flow in the Okavango Delta, Botswana. J. Hydrol. 320 (3–4), 283–301.